

Removal of anionic surfactant from aqueous solutions by adsorption onto biochars: characterisation, kinetics, and mechanism

J. I. Bautista Quispe, L. C. Campos, O. Mašek & A. Bogush

To cite this article: J. I. Bautista Quispe, L. C. Campos, O. Mašek & A. Bogush (22 Jan 2024): Removal of anionic surfactant from aqueous solutions by adsorption onto biochars: characterisation, kinetics, and mechanism, Environmental Technology, DOI: [10.1080/09593330.2024.2304677](https://doi.org/10.1080/09593330.2024.2304677)

To link to this article: <https://doi.org/10.1080/09593330.2024.2304677>



© 2024 The Author(s). Published by Informa UK Limited, trading as Taylor & Francis Group



Published online: 22 Jan 2024.



Submit your article to this journal [↗](#)



Article views: 320



View related articles [↗](#)



View Crossmark data [↗](#)

Removal of anionic surfactant from aqueous solutions by adsorption onto biochars: characterisation, kinetics, and mechanism

J. I. Bautista Quispe^a, L. C. Campos^b, O. Mašek^c and A. Bogush^a

^aCentre for Agroecology, Water and Resilience, Coventry University, Coventry, UK; ^bCentre for Urban Sustainability and Resilience, Department of Civil, Environmental and Geomatic Engineering, University College London, London, UK; ^cUK Biochar Research Centre, School of GeoSciences, University of Edinburgh, Edinburgh, UK

ABSTRACT

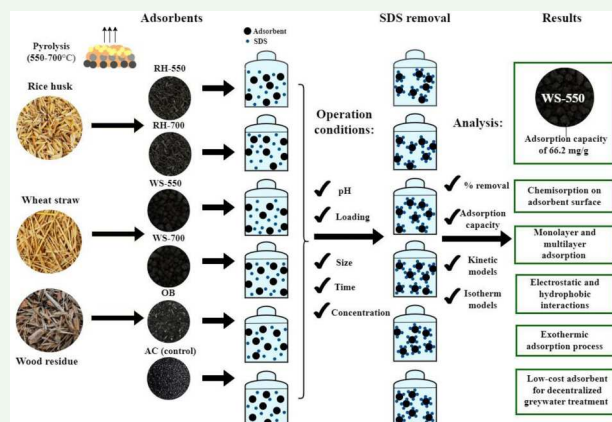
Biochar, a waste biomass-derived adsorbent, holds promise for decentralised wastewater treatment. However, limited research exists on its efficacy in adsorbing anionic surfactants in wastewater. To address this, the adsorption of sodium dodecyl sulphate (SDS), a common anionic surfactant, was studied using various biochar types: rice husk biochar (RH-550 and RH-700), wheat straw biochar (WS-550 and WS-700) produced at 550°C and 700°C, wood-based biochar (OB), and activated carbon (AC) as a control. The study investigated the impact of pH (3–9), adsorbent loading (1–10 g/L), adsorbent size (<0.5–2.5 mm), contact time (5–180 min), and initial concentration (50–200 mg/L) on SDS removal. Under optimised conditions (100 mg/L SDS, 4 g/L adsorbent, 1–2 mm particle size, pH 8.3, and 180 min contact time), maximum SDS removals were RH-550 (78%), RH-700 (82.4%), WS-550 (89.5%), WS-700 (90.4%), AC (97%), and OB (88.4%). Among the tested adsorbent materials, WS-550 exhibited the highest SDS adsorption capacity at 66.23 mg/g compared to AC (80.65 mg/g), followed by RH-550 (49.75 mg/g), OB (45.87 mg/g), RH-700 (43.67 mg/g), and WS-700 (42.74 mg/g). SDS adsorption followed a pseudo-second-order kinetic model, indicating chemisorption on the adsorbent surface. The Freundlich isotherm model exhibited a better fit for the experimental data on SDS adsorption using all tested adsorbents except for RH-550. This study showed that biochars produced from agricultural and forestry residues are effective adsorbents for SDS in aqueous solutions and can be a promising sustainable and low-cost material for the treatment of greywater containing anionic surfactants (e.g. handwashing, laundry, kitchen, and bathroom greywaters).

ARTICLE HISTORY

Received 9 October 2023
Accepted 18 December 2023



KEYWORDS

Biochar; waste-based adsorbent; adsorbent selection; anionic surfactant; SDS removal



Highlights

- Biochar from agricultural and forestry waste can remove SDS from aqueous solution
- Rice husk, wheat straw, and wood biochars removed 78–90.4% of SDS
- Comparable SDS adsorption capacity between WS-550 (66.23 mg/g) and AC (80.65 mg/g)
- SDS removal occurs through monolayer adsorption on the biochar surface
- Biochar can be used for treating domestic greywater with surfactants

CONTACT A. Bogush  ad2855@coventry.ac.uk  Centre for Agroecology, Water and Resilience, Coventry University, Wolston Ln, Ryton-on-Dunsmore, CV8 3LG, Coventry, UK

© 2024 The Author(s). Published by Informa UK Limited, trading as Taylor & Francis Group
This is an Open Access article distributed under the terms of the Creative Commons Attribution License (<http://creativecommons.org/licenses/by/4.0/>), which permits unrestricted use, distribution, and reproduction in any medium, provided the original work is properly cited. The terms on which this article has been published allow the posting of the Accepted Manuscript in a repository by the author(s) or with their consent.

1. Introduction

The largest percentage of chemical products consumed daily are surfactants [1]. It was estimated that the world produced 1.7, 1.8, 9.3, and 13 million tons of surfactant in 1984, 1987, 1995, and 2008, respectively [2,3]. Surfactants are widely used in various applications such as soaps, detergents, emulsifiers, dispersants, lubricants, fabric softeners, wetting agents, and anti-fogging liquids in both industry and domestic settings [4]. Among the various types of surfactants available (e.g. anionic, cationic, non-ionic, and zwitterionic), anionic surfactants account for 65% of the world's total production [4]. There are different types of anionic surfactants, such as linear alkylbenzene sulfonates (LAS), alcohol ether sulphates (AES), secondary alkane sulfonates (SAS), and alcohol sulphates (ALS). Among them, LAS surfactants, such as sodium dodecyl sulphate (SDS), are the most common type of anionic surfactant due to their use in the manufacture of low-cost daily cleaning products [5].

Anionic surfactants have become common constituents in industrial wastewater due to their extensive use [6]. For instance, a high LAS concentration of up to 454 mg/L has been reported in laundry wastewater [7]. Severe environmental and public health consequences occur when untreated wastewater is discharged into water and soil bodies [8]. In aquatic environments, anionic surfactants break down the protective mucus layer that shields fish from parasites and bacteria [9]. By reducing the surface tension of water, anionic surfactants facilitate the adsorption of pesticides by aquatic organisms and increase eutrophication by making pollutants more soluble [8]. Anionic surfactants also pose harm to humans; for instance, the effects of LAS on humans include disruption of the endocrine system, skin irritation, and respiratory problems [10].

Similar to industrial wastewater, domestic greywater generated from bathrooms, washbasins, showers, kitchen sinks, and washing machines also contains anionic surfactants. For instance, Shreya et al. [11] reported concentrations of 118.3, 14.9, and 41.9 mg/L in laundry, shower, and washbasin greywater, respectively. Despite being a significant health and environmental concern, untreated greywater containing high levels of anionic surfactant is commonly reused worldwide for cleaning, toilet flushing, and crop irrigation [12,13]. Therefore, the removal of anionic surfactants from greywater before reuse is crucial to reduce human and environmental risks. Traditional municipal wastewater treatment plants typically employ various physical, chemical, and biological processes to remove anionic surfactants from greywater. However, these

processes are often costly and energy-intensive, limiting their availability in low- and middle-income countries [11]. Consequently, the search for low-cost and sustainable methods to remove anionic surfactants from greywater is essential to enhance its quality and safety for further local reuse [14,15].

Recycling waste materials as wastewater adsorbents has recently gained attention as a strategy to boost industrial symbiosis between the waste and water sectors under the circular economy context [16]. Biochar, a by-product of the thermal decomposition of biomass in the absence of oxygen (pyrolysis), is an example of waste-based adsorbent material of interest for wastewater treatment [17,18]. The physicochemical properties of biochar such as high surface area, high porosity, and presence of reactive surface functional groups have facilitated its use in the treatment of different types of wastewater. For instance, biochar has been used to treat greywater [19], stormwater [20,21], municipal wastewater [22], agricultural wastewater [23], and industrial wastewater [24].

Despite the existing knowledge on the use of biochar in wastewater treatment, little is known about whether biochar is effective in removing anionic surfactants from wastewater. To address this knowledge gap, the objective of this study was to investigate the potential of five different types of biochar produced from rice husk, wheat straw, wood residues, and conventional activated carbon to remove the anionic surfactant SDS under the influence of varying ranges of pH, adsorbent loading, adsorbent size, contact time, and initial concentration. Moreover, this study aimed to explain the possible underlying mechanism involved in SDS adsorption, explicate the nature of the SDS adsorption process, and determine the maximal SDS adsorption capacity for each of the investigated adsorbents. This was achieved through a comprehensive examination of kinetics and adsorption isotherms. Studying the use of biochar to remove anionic surfactant is of great relevance to evaluating its potential as an adsorbent material for on-site wastewater treatment technologies suitable for communities without centralised water treatment systems [17,19].

2. Materials and methods

2.1. Preparation of solution

The following chemicals were used for the experiments: SDS (99%), glacial acetic acid (99.5%), acridine orange (87% dye content), and toluene (99.9%) (Merck, UK). Freshly prepared deionised water was used throughout the experiment. An acridine orange stock solution of 0.005 M was prepared by mixing 0.33 g of acridine

orange with 250 mL of deionised water. A 1000 mg/L SDS solution was prepared in a standard 100 mL volumetric flask. An amount of 100 mg of SDS was weighed using a high-precision electronic balance (PX224, Ohaus, USA) with an accuracy of 0.00001 g. The SDS was poured into the volumetric flask, and then double distilled water was added to complete the solution. A fresh stock solution was prepared every 15 days. After stock solution preparation, different working solutions were obtained with appropriate dilution.

2.2. Adsorbent materials and their characterisation

Standard wheat straw biochar (raw particle size of 5 - 10 mm) and rice husk biochar (raw particle size of 1 - 3 mm), each produced on a pilot-scale pyrolysis unit at 550°C and 700°C, were supplied by the UK Biochar Research Centre (University of Edinburgh, UK) [25]. The standard biochar materials were used in their pure form as received from the UKBRC in sealed containers. Detailed specifications of the material can be found in Table 1. Commercially available 'Oxford biochar', produced from the pyrolysis of mixed forestry residues (mainly wood residues from Beech and Oak trees) at 650°C, was purchased from Oxford Biochar Ltd. [26]. The selection of wheat straw, rice husk, and wood residues as the feedstock material for biochar production was based on their abundance and annual availability as by-products worldwide [27–29]. The choice of biochar samples produced at temperatures above 500°C was made considering the influence of biochar production temperature production to achieve desirable biochar properties (high surface area, high porosity, and abundant active functional groups) for wastewater treatment [25]. Commercially available granular activated carbon (raw particle size of 10 - 20 mm) with a surface area of 1500 - 3000 m²/g was purchased from Tropical Reef (UK). Activated carbon acted as a control adsorbent due to its conventional use and proven capacity to remove SDS from aqueous solutions [30,31].

The rice husk biochars produced at 550°C and 700°C were labelled as RH-550 and RH-700, respectively. The wheat straw biochars produced at 550°C and 700°C were labelled as WS-550 and WS-700, respectively. The biochar made from wood residues and granular activated carbon were labelled as OB and AC, respectively. The adsorbent materials were manually ground using a laboratory mortar and pestle and then sieved to the desired particle size using soil sieves of different mesh sizes. All adsorbents were washed with deionised water to remove any finer foreign material or impurities. After washing, the different types of biochar were dried

at 60°C for 24 h and stored in a desiccator at room temperature.

A BET technique (Nova 4000 analyser, Quantachrome Instruments, USA) was used to determine the surface area of the adsorbent materials. The surface area was calculated using the BET equation from N₂ isotherms (> 99% purity) measured at 77 K [32]. A Fourier transform infrared spectrometer (FTIR) (Nicolet™ iN10 Infrared Microscope, Thermo Scientific, UK) was used to identify the surface functional groups. The scanning range was 675–4000 cm⁻¹. FTIR analyses were performed on the adsorbent materials before and after SDS adsorption to determine changes in the surface functional groups of the adsorbents. The assignment of functional groups corresponding to absorption peaks was based on previous literature [33–35]. The analysis of moisture content, total

Table 1. Characterisation of raw adsorbent materials.

Parameter	Adsorbent				OBa	AC
	RH-550	RH-700	WS-550	WS-700		
Basic utility properties						
BET surface area (m ² /g)	20.10	42	26.40	23.20	300	1500 - 3000
Moisture content (wt %)	1.54	1.49	1.88	2.17	-	-
Total ash (wt%)	47.93	47.93	21.25	23.82	-	-
Volatile matter (wt%)	7.48	4.99	10.55	7.38	-	-
pH	9.71	9.81	9.94	10.03	-	-
pH _{zpc}	7.22	7.64	6.57	6.78	8.70	7.01
Electrical conductivity (dS/m)	0.48	0.69	1.70	1.52	-	-
Biochar C stability (% C-basis)	95.28	100.18	96.51	100.97	N.A.	N.A.
Elemental composition						
C _{tot} (wt%)	48.69	47.32	68.26	69.04	-	-
H (wt%)	1.24	0.63	2.10	1.18	-	-
O (wt%)	2.47	2.06	6.92	5.30	-	-
Mineral N (ammonium & nitrate) (mg/kg)	<3	<3	<3	<3	-	-
Total P (wt%)	0.10	0.16	0.14	0.25	0.06	-
Total N (wt%)	1.04	0.85	1.39	1.32	-	-
Total K (wt%)	0.39	0.62	1.56	1.47	0.17	-
As (mg/kg dry wt)	0.26	bdl	1.16	1.26	-	-
Cd (mg/kg dry wt)	17.84	19.97	3.15	1.27	-	-
Cr (mg/kg dry wt)	4.99	bdl	bld	4.45	-	-
Co (mg/kg dry wt)	2.94	4.59	1.14	1.58	-	-
Cu (mg/kg dry wt)	5.40	26.93	3.63	4.68	7.65	-
Pb (mg/kg dry wt)	bdl	bdl	bdl	bdl	-	-
Hg (mg/kg dry wt)	bdl	bdl	bdl	bdl	-	-
Mo (mg/kg dry wt)	0.64	0.67	0.84	3.26	-	-
Ni (mg/kg dry wt)	3.00	2.71	1.00	2.50	-	-
Se (mg/kg dry wt)	bdl	bdl	bdl	bdl	-	-
Zn (mg/kg dry wt)	23.58	36.17	10.50	12.03	35.5	-
Production parameters						
Temperature (°C)	550	700	550	700	650	-
Heating rate (°C/min)	98	92	80	79	-	-
Biochar yield (wt%)	37.20	32.77	24.11	23.54	-	-
Kiln residence time (min)	15	17	15	15	-	-

bdl: below detection limit; N.A.: not applied

ash, and volatile matter was carried out by a thermogravimetric analyser (Mettler-Toledo TGA/DSC1, Mettler Toledo, USA). The primary elemental composition of the materials (C and H) was analysed using an elemental analyser (Flash 2000, CE Elantech Inc, New Jersey, USA). The O content was determined by difference. Biochar pH and electrical conductivity were determined using benchtop probes (Mettler-Toledo, USA) to measure the pH and electrical conductivity of solutions composed of 1 g of biochar and 20 mL of deionised water. Solutions were shaken for 1.5 h in an Orbital Multi-Platform Shaker PSU-20i (Grant Instruments Ltd, UK) before measurement of pH and electrical conductivity [36]. The determination of the point of zero charge (pH_{zpc}) involved adjusting the initial pH of solutions (biochar dosage: 10 g/L) using sodium hydroxide (NaOH) and nitric acid (HNO₃) solutions within the range of 3 - 13. Subsequently, the final pH values were measured after shaking the solutions for 24 h at 120 rpm [37]. The biochar C-stability was assessed through the accelerated ageing method, employing a combination of thermal and chemical oxidation. Total P and total K were determined using Aqua Regia digestion, followed by ICP (Inductive Coupled Plasma). The analysis of heavy metals involved the modified dry ashing method, followed by ICP-OES (Optical Emission Spectrometry). All characterisation analyses were performed at the UK Biochar Research Centre (University of Edinburgh, UK), except for the FTIR analysis. The FTIR analysis and all further experimental analyses were carried out at the High-performance Analytical Hub at the Centre for Agroecology, Water and Resilience (Coventry University).

2.3. Experimental procedure

2.3.1. Influence of operation parameters on SDS adsorption

Adsorption experiments were carried out in 100 mL test bottles containing 50 mL of SDS stock solution and a known concentration and amount of biochar sample. The test bottles were shaken in an orbital shaker Mega-fuge 16R (Thermo Scientific, Germany) at 200 rpm for a predetermined time (5 - 180 min). Rotation was kept constant throughout the experimental work. After shaking, the solution was filtered through a Whatman filter paper, and the filtrate was centrifuged at 5000 rpm for 10 min. Each trial was conducted in triplicate to ensure the accuracy of the results.

The influence of pH (range 3 - 9), adsorbent loading (range 1 - 10 g/L), adsorbent size (< 0.5, 0.5 - 1, 1 - 2, and 2 - 2.5 mm), initial SDS concentration (range 50 - 200 mg/L), and contact time (range 5 - 180 min) on the extent of SDS adsorption was investigated. For the

trials evaluating the influence of the pH range on SDS adsorption, the test bottles contained 50 mL of 100 mg/L SDS solution, 4 g/L of adsorbent loading, and adsorbent particle size of 1–2 mm. The pH value of the SDS solution was adjusted to 3, 5, 7, and 9 by adding either 0.1 M of hydrochloric acid (HCl) or 0.1 M of NaOH. For the trial evaluating the influence of adsorbent loading range on SDS adsorption, the test bottles contained 50 mL of 100 mg/L SDS and adsorbent particle size of 1–2 mm. The adsorbent loadings under study were 1, 2, 4, 6, 8, and 10 g/L. For the trial assessing the influence of adsorbent size on SDS adsorption, the test bottles contained 50 mL of 100 mg/L SDS and 4 g/L of adsorbent loading. The particle sizes under study were < 0.5, 0.5–1, 1–2, and 2–2.5 mm. For the trial studying the impact of initial SDS concentration on SDS adsorption, the test bottles contained 50 mL of solution, 4 g/L of adsorbent loading, and an adsorbent particle size of 1–2 mm. The initial SDS concentrations were 50, 100, 150, and 200 mg/L. For the trial evaluation of the effect of contact time on SDS adsorption, the test bottles contained 50 mL of 100 mg/L SDS solution, 4 g/L of adsorbent loading, and adsorbent particle size of 1–2 mm. The contact times were 5, 10, 30, 60, 90, 120, 150, and 180 min. The pH value of the SDS solution for most experiments (excluding the first experimental trials) was 8.3, the natural pH value of the solution. The pH value of the SDS solution was not adjusted because findings from the pH influence trials showed negligible pH impact on the extent of SDS removal. The contact time for most experimental trials (excluding the last one) was set to 180 min. All batch experiments were performed at room temperature (20 °C).

2.3.2. Kinetic and isotherm experiments

Kinetic and isotherm experiments were conducted by placing 4 g/L of adsorbent with a particle size of 1–2 mm to 50 mL of SDS solutions at various concentrations (50, 100, 150, and 200 mg/L) inside 100 mL test bottles. The contact time was set at 180 min, which was sufficient to reach equilibrium. The experiments were carried out at room temperature. Initial concentrations of SDS surfactant were chosen based on those commonly found in greywater effluents [11,38].

2.4. Experimental analysis

The concentration of SDS in both the feed and filtrate solution from centrifugation was measured using the acridine orange complex method [39,40]. Anionic surfactants, such as SDS, form a complex with cationic dyes (e.g. acridine orange) known as the ion-association complex. This complex can be extracted in an organic

solvent layer such as toluene, under low pH conditions achieved by adding glacial acetic acid. Samples were diluted to create a 10 mL sample within the recommended concentration range of 1 - 6 mg/L for SDS analysis [39,40]. The solution was then transferred into a 50 mL glass vial, and 100 μ L of acridine orange, 100 μ L of glacial acetic acid, and 5 mL of toluene were added. Subsequently, the contents were shaken for 2 min and allowed to settle for 5 min. Using a laboratory pipette, approximately 2.5 mL of the toluene layer was transferred into a 3 mL test cuvette. The surface of the test cuvette was then cleaned with ethanol (99%) and used directly for absorbance measurement at λ_{max} of 467 nm using the spectrophotometer WPA S800+ (Biochrom, USA). For the determination of the SDS concentration after adsorption experiments, a calibration curve and equation were created initially by measuring the absorbance of standard SDS solutions at concentrations of 1, 2, 3, 4, 5, and 6 mg/L. Subsequently, the values obtained from the absorbance measurement of the test cuvettes were substituted into the calibration curve equation to determine the final SDS concentration. The amount of SDS adsorbed onto the adsorbents at time t , q_t (mg/g) was determined using Equation (1) while the SDS removal efficiency of adsorption was calculated using Equation (2). C_0 is the initial SDS concentration (mg/L), C_t is the SDS concentration at any time t , v is the volume of the SDS solution (L) and m is the mass of adsorbent (g).

$$q_t = ((C_0 - C_t)/m) \times v \quad (1)$$

$$\% \text{ Adsorption} = ((C_0 - C_t)/C_0) \times 100 \quad (2)$$

2.5. Statistical analysis

The mean and standard deviation values of SDS removal efficiency (%) and maximal SDS adsorption capacity (mg/g) for each of the investigated adsorbents were calculated. A two-way ANOVA test was conducted to assess the main effect of the operation conditions (pH, adsorbent loading, adsorbent size, contact time, and initial concentration) and the types of adsorbents on the removal of SDS. The significance level for the statistical tests was 5% ($P < 0.05$).

3. Results and discussion

3.1. Characterisation of biochar adsorbents

Table 1 shows the properties and production parameters of the adsorbents [25,26,41]. The BET surface area of the biochar adsorbents ranged from 20.10 m^2/g for RH-550

to 300 m^2/g for OB. Generally, biochar adsorbents derived from the pyrolysis of agricultural residues, such as rice husk (RH-550 and RH-700) and wheat straw (WS-550 and WS-700), exhibited lower surface areas compared to biochar produced from wood residues (OB). Commercial AC displayed the highest surface area (1500–3000 m^2/g). The ash content varied from 21.25 wt% in WS-550 to 47.93 wt% in RH-550 and RH-700. The pH value of the biochar adsorbents was alkaline, ranging from 9.71 for RH-550 to 10.03 for WS-700. The biochar adsorbents demonstrated a high degree of carbonisation, with the total carbon (C_{tot}) content being higher in the wheat straw biochars ($\sim 70\%$) than in the rice husk biochars ($\sim 50\%$). The FTIR spectra of the biochar adsorbents and AC are depicted in Figure 1. The adsorbents exhibited functional groups such as -O-H stretching vibrations at a wavenumber of $\sim 3670 \text{ cm}^{-1}$; C-H bond stretching in aliphatic formation at $\sim 3070 \text{ cm}^{-1}$; C=O stretching of carboxylic, ester, ketone and aldehyde groups at $1670\text{--}1870 \text{ cm}^{-1}$; -C=C- stretching of the aliphatic group at $\sim 1570 \text{ cm}^{-1}$, and C-O stretching of the aliphatic group at $\sim 1270 \text{ cm}^{-1}$. Notably, RH-550, WS-550, OB, and AC displayed more surface functional groups than the other adsorbents. Strong peaks of -O-H, C-H, C=C, and =C-H groups were observed for AC, WS-550, and OB. In contrast, RH-700 and WS-700 exhibited fewer surface functional groups. Elnour et al. [42] demonstrated that the functional groups of biochar samples decreased with increased pyrolysis temperature, possibly due to the destruction of functional groups during the higher-temperature carbonisation process. Peaks of C=C, C-O-C, and =C-H groups were observed for RH-700, while peaks of C=C and =C-H groups were reported for WS-700.

3.2. Effect of pH on SDS adsorption

The pH of the solution influences the surface charge of the adsorbent, and any variations in pH are anticipated to impact the extent of adsorption. Usually, adsorbents with higher pHzpc values can be employed for the adsorption of anionic surfactants, as their surfaces become positively charged when the solution pH is below their pHzpc values [37]. To investigate the pH-dependent impact on SDS adsorption, solutions with the pH values of 3, 5, 7 and 9 were employed. As depicted in Figure 2, variations in solution pH did not exert a significant effect on SDS removal ($P > 0.05$). When the solution pH was below the pHzpc value of the tested adsorbents (RH-550: 7.22, RH-550: 7.64, WS-550: 6.57, WS-700: 6.78, AC: 7.01, and OB: 7.8), the adsorbent surfaces exhibited a positive charge, facilitating

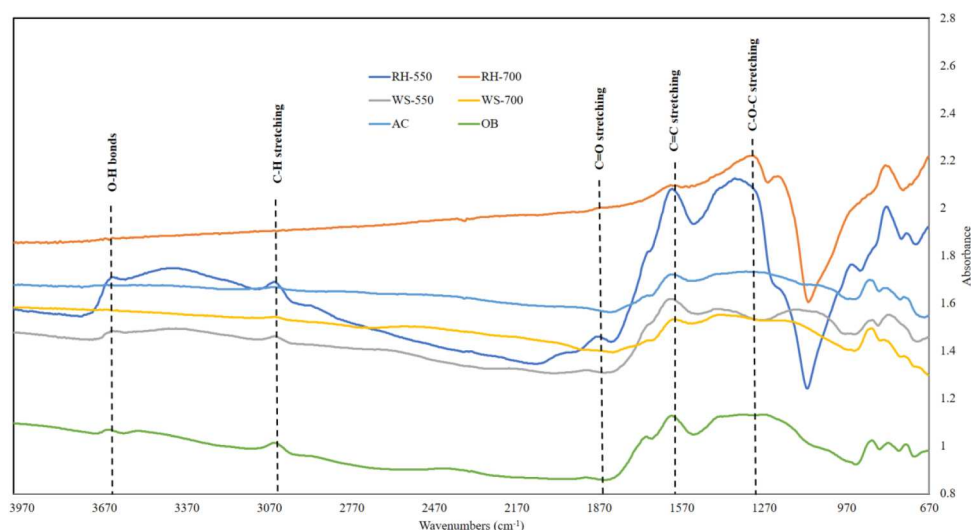


Figure 1. FTIR spectra of the raw adsorbent materials.

SDS adsorption through electrostatic interactions between the adsorbent and the anionic surfactant (Table 1). Interestingly, when the solution pH was higher than the pHzpc value, there was no anticipated decrease in SDS adsorption for rice husk biochars (RH-550 and RH-700); instead, SDS adsorption levels remained consistent. This trend was observed similarly for wheat straw biochars (WS-550 and WS-700), where SDS adsorption tended to increase as expected when the solution pH was below or close to the pHzpc, but it slightly decreased at a solution pH of 9. Regarding AC, SDS adsorption increased at solution pH values lower than the pHzpc value and showed a slight decrease at solution pH values higher than the pHzpc value. Conversely, for OB, there were no notable changes in SDS adsorption across the various tested solution pH values. Overall, SDS removal percentages were observed in the range of 76.5% to 77.4%, 76.6% to 80%, 81.5% to 87.5%, 82.1% to 87.9%, 89.2% to 96.3% and

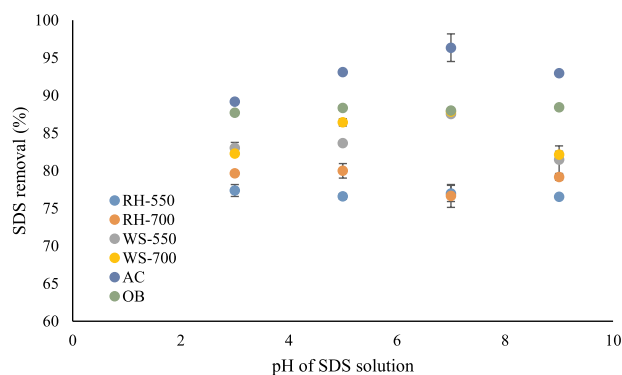


Figure 2. Effect of pH on SDS removal. Some error bars are smaller than the symbol size.

87.7% to 88.4% for RH-550, RH-700, WS-550, WS-700, AC, and OB, respectively, across a pH range of 3–9. While pH variations were expected to predominantly control SDS adsorption through electrostatic interactions, the lack of pH dependency in SDS removal suggested the influence of additional removal mechanisms. As identified by Pavan et al. [43] and Nowrouzi et al. [44], six mechanisms are associated with surfactant adsorption, including ion exchange, ion pairing, hydrogen bonds, π -electron polarisation, dispersion forces, and hydrophobic interactions. For example, the adsorption of sodium lauryl sulphate (SLS) on commercial AC demonstrated a reliance on hydrophobic interactions, as reported by Bindaes & Franco [45]. It was reported that SLS adsorption relied mainly on hydrophobic interactions between the surface of AC and the hydrophobic tail of the surfactant. Similarly, Schouten et al. [46] investigated the adsorption of LAS from laundry rinsing water on AC and found that the interaction between the hydrophobic LAS alkyl chain and the aromatic group with the hydrophobic AC surface was the main LAS removal mechanism. However, Sen et al. [47] reported a pH-dependent SDS removal by pine cone biomass, suggesting that electrostatic interactions could control SDS adsorption. This means that the dominant SDS removal mechanism might be different according to the chemical nature of the surfactant, the surface properties of the adsorbent material, and the characteristics of the aqueous solution.

The study of the effect of pH on the extent of SDS adsorption was coupled with an investigation into the effect of pH on contact time. Fig. S1 illustrates that, under the tested conditions, the maximum adsorption capacity of the adsorbents was achieved within the initial 30 min,

becoming negligible after 120 min (supplementary information). Similar to SDS removal, no significant differences in the adsorption capacity were observed among the adsorbents. AC exhibited the highest adsorption capacity (24.4 mg/g) followed by OB (22.1 mg/g), WS-700 (22.0 mg/g), WS-550 (21.9 mg/g), RH-700 (20 mg/g), and lastly by RH-550 (19.3 mg/g). Several studies evaluating the influence of pH on adsorption capacity have been reported in the literature. Than et al. [48] reported maximum adsorption capacities of 68.54 mg/g (pH 3) and 57.92 mg/g (pH 6) for thermally activated (400 - 1000°C) fish scale (RFSP) and seashell powder (RSSP), respectively. Bhandari & Gogate [49] found a maximum adsorption capacity of 28.57 mg/g for sodium dodecyl benzene sulfonate (SDBS) using phosphoric acid-activated crushed coconut shell at a solution pH of 2. The adsorption capacities found for biochars in this study were lower compared to the reported literature. However, by comparing the maximum adsorption capacity data reported by Bhandari & Gogate [49] with those of biochar adsorbents discussed in this paper, it can be assumed that biochar adsorbents can be considered an alternative to the chemically-activated adsorbents. As pH exhibited an overall negligible impact on SDS removal, subsequent trials were conducted at the natural pH of the solution (8.3).

3.3. Effect of adsorbent loading on SDS adsorption

The extent of SDS adsorption depends on the amount of adsorbent used in this study. To understand the effect of adsorbent loading on the extent of adsorption, different amounts of adsorbents within the range of 1, 2, 4, 6, 8, and 10 g/L were used in the experiments (Figure 3). As shown in Figure 3, both the type of adsorbent and the adsorbent loading significantly affected the removal of

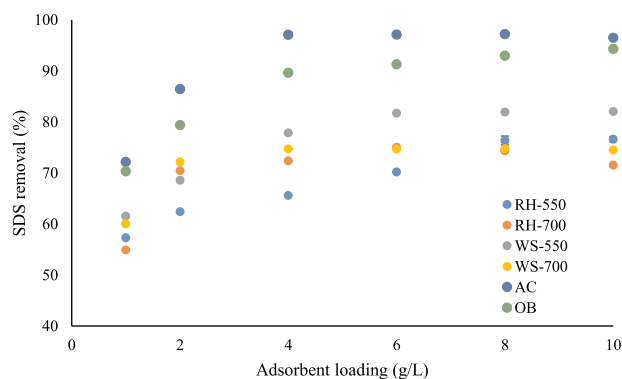


Figure 3. Effect of adsorbent loading on SDS removal. Error bars are smaller than the symbol size.

SDS ($P < 0.05$). For instance, SDS removal increased from 57.3% to 76.6%, 54.9% to 75.0%, 61.5% to 82%, 60% to 74.7%, 72.2% to 97.2%, and 70.3% to 94.3% for RH-550, RH-700, WS-550, WS-700, AC, and OB, respectively. This trend may be attributed to the increased availability of adsorption sites. Additionally, the increased dosage of adsorbent also increased exchangeable sites, resulting in more efficient adsorption. Overall, an increase in the adsorbent amount above 6 g/L did not yield beneficial results. In fact, SDS removal was slightly reduced for additional loading above 8 g/L on the RH-550, RH-700, WS-700, and AC trials. It is possible that the aggregation of particles and shielding of active sites explain the observed reduction in removal at higher loadings. The results reported in this study were similar to those reported by Bhandari & Gogate [49], who showed an increase in SDBS removal by up to 92.5% using 3 g/L of adsorbent dosage (activated coconut shell). Likewise, Mi-na et al. [50] concluded that utilising 4 g/L of chromium leather waste as an adsorbent material is enough to remove 95% of SDBS from a 100 mg/L initial concentration. In the literature, however, studies have shown that much larger dosages of adsorbent enhanced anionic surfactant removal. For instance, Ersa et al. [51] established that LAS removal decreased at a larger dosage of adsorbent. When the dosage of rice straw increased from 10 to 20 g/L, the LAS removal decreased from 70% to 50%. In another study, 10 g/L of a polymeric composite supported with activated rice husk removed 96% of detergent (MBAS) from greywater [52]. From the results obtained and the information reported in the literature, it was not possible to establish a one-way effect of the adsorbent dosage on the surfactant removal extension. This is due to the differences in anionic surfactant type and adsorbent materials used in the present study compared to others reported in the literature. In the case of biochar performance, even though SDS removal was above 70% for all the investigated biochar adsorbents in this study, it is not possible to compare their performance in removing surfactants in real or synthetic wastewater due to a lack of studies.

The study of the combined effect of adsorbent dosage and contact time on the extent of adsorption capacity was also investigated in the present study. Fig. S2 illustrates the variations in adsorption capacity obtained with each adsorbent (supplementary information). It can be noticed that the adsorption capacity increased during the first 30 min of contact and became negligible after 60 min for most of the adsorbents. As expected, the adsorption capacity increased as the dosage of the adsorbent increased. Similar maximum adsorption capacities were observed when

the adsorbent dosage was between the range of 1 to 6 g/L, particularly for RH-700 (Fig. S2b), WS-550 (Fig. S2c), WS-700 (Fig. S2d), AC (Fig. S2e), and OB (Fig. S2f). This agrees with the results shown in Figure 3 where negligible SDS removal percentages were reported for adsorbent loading above 6 g/L for all the tested adsorbents. In the literature, similar studies have found a contradictory relationship between adding larger adsorbent loadings and their effect on the removal of surfactants. For instance, the results obtained in this study seem to be consistent with Gupta et al. [53], who found an increase in the adsorption capacity when dosages of waste-activated carbon were increased from 0.1 to 6 g/L. As previously mentioned, the increased adsorption capacity was attributed to the increased number of sites available for adsorption. In contrast to previous findings, Sen et al. [47] described that a decrease in the amount of adsorbed SDS from 71.54 to 26.55 mg/g was observed when the adsorbent dosage (pine cone biomass) increased from 0.02 to 0.04 g. The decrease in SDS adsorbed was due to a split in flux or the concentration gradient between the concentration of the solute in the solution and the concentration of the solute on the adsorbent surface. In addition, a similar trend was noted by Purakayastha et al. [54] when dosages of rubber granules in the range of 5 to 15 g/L were used to remove SDS. These different results suggest that SDS removal depends not only on the adsorbent amount but also on the surface properties of the adsorbents.

3.4. Effect of adsorbent particle size on SDS adsorption

Various sizes of adsorbents within the ranges of < 0.5, 0.5–1, 1–2, and 2–2.5 mm were employed in the experiments to investigate the influence of adsorbent size on the extent of SDS adsorption. Figure 4 shows the experimental data on SDS removal under the influence of

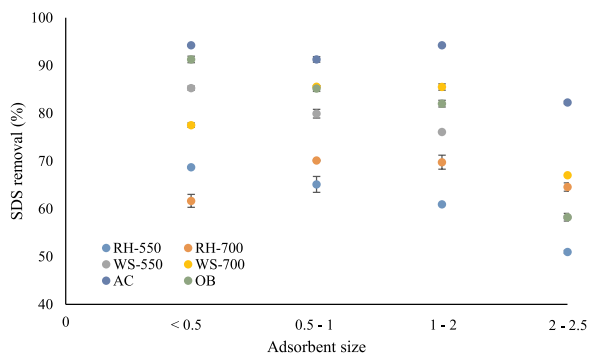


Figure 4. Effect of the adsorbent particle size on SDS removal. Some error bars are smaller than the symbol size.

adsorbent particle size. The removal of SDS decreased for RH-550, WS-550, and OB when the adsorbent particle size increased from < 0.5 to 2.5 mm (Figure 4). For instance, the removal of SDS decreased from 68.7% to 51%, 85.3% to 58.2%, and 91.3% to 58.2% for RH-550, WS-550 and OB, respectively. However, for RH-700, WS-700 and AC, the SDS removal did not follow a decreasing trend as the adsorbent particle size increased. Overall, SDS removal was not significantly affected by the adsorbent particle size or the type of adsorbent used ($P > 0.05$).

Several studies have reported a similar trend in the removal of SDS when the adsorbent size was increased. Purakayastha et al. [54] observed a high uptake of SDS of 90%, 86%, and 84% for average particle sizes of 75, 150 and 425 μm , respectively. Similarly, Ersa et al. [51] assessed the effect of different particle sizes retained at 50 (0.3 mm) 100 (0.15 mm), and 140 mesh (0.1 mm) on SDS removal. SDS was effectively removed when the particle size was smaller. Since adsorption is a surface phenomenon, a higher SDS removal percentage is observed as the size of the particles decreases. This is because the surface area increases as the particle size decreases [54]. In the case of RH-700 and WS-700, the SDS removal gradually increased to 69.8% and 85.5%, respectively, with an increase in adsorbent size from < 0.5 to 2 mm, after which it slightly decreased to 64.6% and 67%, respectively. Enaime et al. [17] claimed that biochar produced at higher temperatures than 500°C exhibited a high degree of hydrophobicity and a high micropore volume, making the adsorbent highly effective for removing organic pollutants such as SDS. It seems that increasing the particle size of RH-700 and WS-700 resulted in higher micropore volume, facilitating hydrophobic interactions, as explained in Section 3.1. For AC, above 90% of SDS removal was reported for the adsorbent sizes within the range of < 0.5 to 2 mm, followed by an SDS removal decrease to 82.3% for the adsorbent size of 2 - 2.5 mm. Overall, particles larger than 2 mm might negatively affect SDS removal due to a decrease in adsorbent surface area. Therefore, an adsorbent particle size of 1 - 2 mm was used for further trials.

Turning now to the adsorption capacities observed for each adsorbent, AC, OB, WS-700, WS-550, RH-700, and RH-550 removed 23.6, 22.8, 21.4, 21.3, 17.5, and 17.2 mg/g, respectively. Compared to literature reports, the adsorbents examined in this study exhibited significantly higher adsorption capacities. For instance, Purakayastha et al. [54] reported an adsorption capacity of 0.5 mg/g for rubber granules of different particle sizes. Similarly, Ersa et al. [51] demonstrated a maximum adsorption capacity of 0.37 and 0.62 mg/g for eggshell

and rice straws, respectively. The low adsorption capacity reported for rice straws (0.62 mg/g) compared to the values obtained in this study for rice husk biochar (49.75 mg/g for RH-550 and 43.67 mg/g for RH-700) can be explained by the differences in surface area between the two adsorbents. It is believed that biomass thermal treatment (pyrolysis) at 550 - 700°C increased the biochar surface area [55]. For example, the surface area was 22.35 and 42 m²/g for rice straws and rice husk biochar thermally activated at 700°C [51], respectively (Table 1). This suggests that biochars may be more efficient at removing SDS than adsorbents based on raw biomass.

3.5. Effect of contact time on SDS adsorption

Time is a critical factor in adsorbate–adsorbent interaction during adsorption. Generally, a larger number of vacant sites are available at the beginning of the process, resulting in a faster rate of adsorption [49,56]. However, a decline in the concentration gradient, a reduction in vacant sites, and unfavourable interactions between adsorbed molecules and molecules in the solution cause the rate of adsorption to decrease over time. Hence, studying the effect of contact time on the extent of SDS adsorption is crucial to establish batch cycle timings that allow maximum removal and assess the adsorption equilibrium characteristics. Figure 5 illustrates the variation of SDS removal with time. In general, contact time and the type of adsorbent significantly affected SDS removal ($P < 0.05$). As can be observed for all adsorbents, the uptake of SDS from the solution exceeds 50% within the first 10 min. Around 72.8%, 79.5%, 83.5%, 74.8%, 67.4%, and 63% SDS removal was obtained for RH-550, RH-700, WS-550, WS-700, AC, and OB, respectively, after 10 min of contact time. The

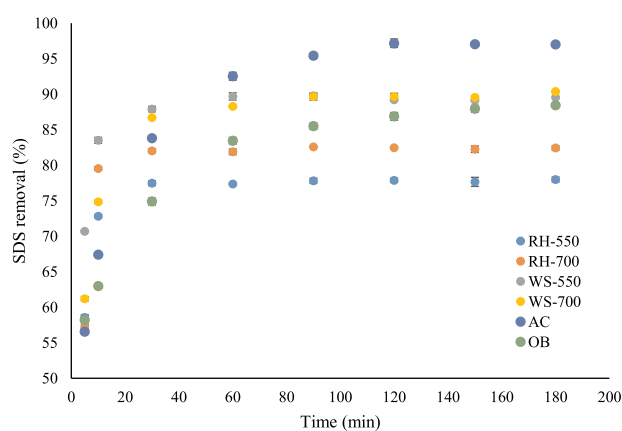


Figure 5. Effect of contact time on SDS removal. Some error bars are smaller than the symbol size.

rapid SDS uptake at the beginning of the process can be attributed to the abundance of vacant adsorption sites on the surface of the adsorbents, which gradually decreased over time until maximum SDS removal is achieved. Overall, the maximum SDS removal for RH-550, RH-700, WS-550, WS-700, AC, and OB was 78%, 82.4%, 89.5%, 90.4%, 97%, and 88.4%, respectively. Among the adsorbents, the time required for SDS removal to become negligible varied. For instance, the adsorption equilibrium time for RH-550, RH-700, WS-550, WS-700, AC, and OB was 30, 60, 60, 120, and 90 min, respectively. This means that despite AC and OB being among the adsorbents with the highest SDS removal at equilibrium time, the physicochemical properties of RH-550, RH-700, WS-550, and WS-700 (e.g. surface area) seem to favour the SDS uptake at a faster rate than AC and OB.

Various studies have examined how contact time affects anionic surfactant adsorption. Kochkodan et al. [57] reported an equilibrium adsorption time of 24 h for the removal of SDBS using carbon black as the adsorbent. Ncibi et al. [58] investigated the adsorption of SDBS on As-synthesised multiwalled carbon nanotubes and reported an equilibrium adsorption time of 100 min. A similar equilibrium time of 120 min for SDBS adsorption with AC was obtained in Valizadeh et al. [59] and the present study. Physical and biological adsorption has also been used to remove SDBS, however, a long equilibrium time of 250 h has been reported [60]. Overall, it can be stated that biochars require less time to reach equilibrium than other adsorbents reported in the literature. As shown in Figure 5, although the maximum SDS removal by the adsorbents under study occurred after 120 min, isotherm tests were performed for 180 min to ensure that the concentration at equilibrium was achieved for all the adsorbents under study.

3.6. Effect of initial SDS concentration on SDS adsorption

The extent of removal and adsorption capacity depends on the initial SDS concentration. This is because mass transfer from the bulk to the surface of an adsorbent is determined by the concentration of the adsorbate solution [61]. In this study, the effect of four initial SDS concentrations (50, 100, 150, and 200 mg/L) on SDS adsorption was studied. Figure 6 depicts the influence of the initial SDS concentration on the extent of SDS removal. SDS removal was significantly affected by both initial concentration and adsorbent type ($P < 0.05$). Overall, the SDS removal decreased when the initial concentration increased for adsorbents. For

instance, at an initial SDS concentration of 50 mg/L, the SDS removal was reported above 92% for all adsorbents. However, it dropped gradually to 42.9%, 41.4%, 55.6%, 47.5%, 89.5%, and 43.5% for RH-550, RH-700, WS-550, WS-700, AC, and OB, respectively. When compared to biochars, there was not much reduction for SDS removed by AC. A possible explanation for this is that AC has a much higher surface area (1500 - 3000 m²/g) than the rest of the adsorbents, which allows the presence of more active adsorption sites to favour the adsorption process [17]. However, Figure 7 shows that adsorption capacity increased as the initial concentration increased. Adsorption capacities increased from 10.54 to 35.74 mg/g, 11.17 to 35.34 mg/g, 11.06 to 38.90 mg/g, 11.71 to 36.87 mg/g, 12.14 to 47.38 mg/g, and 10.94 to 35.88 mg/g for RH-550, RH-700, WS-550, WS-700, AC, and OB, respectively. Fig. S3 shows that the adsorbents reached their maximum SDS adsorption capacities within the first 30 min of the treatment time (supplementary information). Increasing the probability of collision and increasing the driving force for mass transfer may have contributed to high adsorption capacity under high initial SDS concentrations [62,63]. Several studies have described similar effects of initial concentration on adsorption capacity. Bhandari & Gogate [49] reported an increase in the adsorption capacity from 20 to 75 mg/g when the initial SDS concentration increased from 40 to 160 mg/L. A similar increase from 56.81 to 74.62 mg/g in the adsorption capacity of pinecone biomass was demonstrated for an increase in SDS initial concentration from 20 to 70 mg/L [47]. This indicates that biochars can remove SDS even when exposed to aqueous solutions containing high SDS concentrations (> 150 mg/L). This suggests they might hold the potential to treat different types of greywater such as shower, laundry, handwashing, and kitchen wastewater, which have anionic surfactant

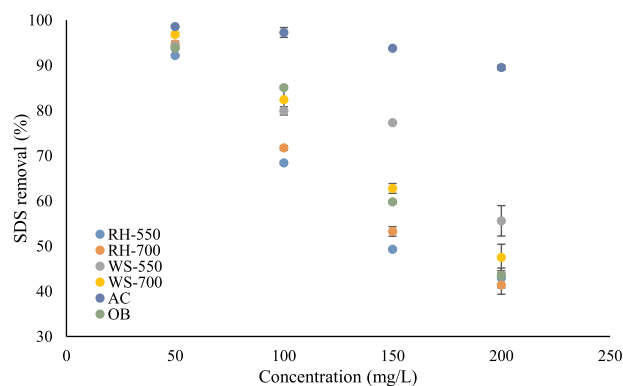


Figure 6. Effect of initial SDS concentration on SDS removal. Some error bars are smaller than the symbol size.

concentrations in the range of 14.9, 101.4, 41.9, and 26.5 mg/L, respectively [38].

3.7. Kinetic study

Kinetic studies provide valuable information on the adsorption mechanism [49]. An understanding of adsorption kinetics is useful for designing large-scale adsorption columns and determining the dynamic behaviour of adsorption systems [64]. The adsorption and accessibility to site adsorption at the solid-liquid interface generally occur in the following steps: bulk diffusion, external diffusion, intraparticle diffusion, and interaction with the surface sites [65]. The most common kinetic models, the pseudo-first-order, pseudo-second-order, and intraparticle diffusion models were used in the study to determine the mechanism of adsorption.

3.7.1. Pseudo-first-order model

Lagergren's kinetic equation, also known as the pseudo-first-order equation, was used to fit the data. According to the pseudo-first-order model, the rate of adsorption site occupation is proportional to the number of unoccupied sites [66]. Generally, if adsorption takes place through diffusion through an interface, then it follows Lagergren's pseudo-first-order rate equation [65]. Equation (3) provides the linearised mathematical form of the model where q_e (mg/g) and q_t (mg/g) represent the amount of SDS adsorbed (mg/g) onto the adsorbents at equilibrium and at any time t (min), respectively. The parameter k_1 is the pseudo-first-order rate constant (1/min). For each of the adsorbents under evaluation, a plot of $\ln(q_e - q_t)$ versus t was created, and a linear regression equation was derived from data fitting to calculate the values of k_1 and q_e (denoted as $q_{e(cal)}$) from the slope and the intercept, respectively. The determination coefficient (R^2) was calculated to assess the

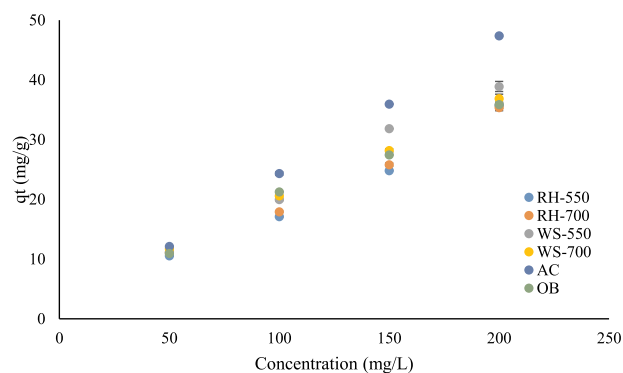


Figure 7. Effect of initial SDS concentration on adsorption capacity (q_t). Some error bars are smaller than the symbol size.

suitability of the kinetic model for the experimental data.

$$\ln(q_e - q_t) = \ln q_e - k_1 t \quad (3)$$

Based on the data presented in Fig. S4, the average values of R^2 were calculated as 0.740, 0.753, 0.826, 0.850, 0.836, and 0.870 for RH-550, RH-700, WS-550, WS-700, AC, and OB, respectively (supplementary information). Overall, the low values of R^2 indicated that the adsorption experimental data for the six adsorbents do not fit the pseudo-first-order kinetic model. This is further supported by the comparison between the experimental and calculated values of q_e denoted as $q_{e(\text{exp})}$ and $q_{e(\text{cal})}$, respectively (Table 2). A significant difference between $q_{e(\text{exp})}$ and $q_{e(\text{cal})}$ for initial SDS concentrations of 50, 100, 150, and 200 mg/L can be observed for all tested adsorbents. For instance, $q_{e(\text{exp})}$ values for RH-500 were 7.70, 17.97, 25.70, and 35.70 mg/g for initial SDS concentrations of 50, 100, 150, and 200 mg/L, respectively. The $q_{e(\text{cal})}$ values obtained after fitting the data to the pseudo-first-order model for similar concentrations were 1.52, 3.68, 0.93, and 0.35 mg/g, respectively. Similar trends were observed for RH-700, WS-550, WS-700, AC, and OB. Overall, based on the principles of the pseudo-first-order model, it can be inferred that the SDS mechanism does not occur via diffusion through an interface.

3.7.2. Pseudo-second-order model

The pseudo-second-order model assumes that the adsorption mechanism is through the process of

chemisorption where adsorbate molecules (e.g. SDS) are chemically bound to active sites located on the surface of the adsorbents [59]. The linearised form of the pseudo-second-order kinetic model is expressed in Equation (4), where q_e (mg/g) and q_t (mg/g) are the amounts of SDS adsorbed (mg/g) onto the adsorbents at equilibrium and at any time t (min), and k_2 is the pseudo-second-order rate constant (g/mg·min). A plot of t/q_t versus t was created, and a linear regression equation was calculated from data fitting to obtain values of k_2 and $q_{e(\text{cal})}$ from the slope and the intercept, respectively. Similar to Section 3.7.1, the values of R^2 were calculated to determine the suitability of the kinetic model for the experimental data.

$$t/q_t = 1/k_2 q_e^2 + (1/q_e)t \quad (4)$$

Fig. S5 depicts the pseudo-second-order kinetic plots for the used adsorbents along with the corresponding R^2 values (supplementary information). In contrast to the pseudo-first-order model, the average value of R^2 was much closer to 1 for most adsorbents. For example, average R^2 values of 0.998, 0.999, 0.999, 0.999, 1, and 0.984 were reported for RH-550, RH-700, WS-550, WS-700, AC, and OB, respectively. Additionally, as can be seen from Table 3, the values of $q_{e(\text{exp})}$ and $q_{e(\text{cal})}$ for the initial concentrations of 50, 100, 150, and 200 mg/L are closer to each other for all used adsorbents. For instance, $q_{e(\text{cal})}$ values for RH-550 were 8.08, 18.24, 25.77, and 35.71 mg/g for initial concentrations of 50, 100, 150, and 200 mg/L, respectively. According to the obtained pseudo-second-order model, the $q_{e(\text{exp})}$

Table 2. Kinetic parameters for the pseudo-first-order model.

Adsorbent	Parameter	C_0 (mg/L)			
		50	100	150	200
RH-550	$q_{e(\text{exp})}$ (mg/g)	7.70	17.97	25.70	35.70
	$q_{e(\text{cal})}$ (mg/g)	1.52	3.68	0.93	0.35
	k_1 (1/min)	0.0002	0.0002	0.0001	0.0001
	R^2	0.736	0.903	0.486	0.769
RH-700	$q_{e(\text{exp})}$ (mg/g)	11.38	18.15	25.26	35.41
	$q_{e(\text{cal})}$ (mg/g)	0.87	1.76	1.27	0.37
	k_1 (1/min)	0.0002	0.0002	0.0001	0.0002
	R^2	0.777	0.716	0.661	0.858
WS-550	$q_{e(\text{exp})}$ (mg/g)	11.17	19.80	30.12	39.21
	$q_{e(\text{cal})}$ (mg/g)	0.13	0.59	1.22	0.95
	k_1 (1/min)	0.0001	0.0002	0.0002	0.0002
	R^2	0.913	0.625	0.912	0.855
WS-700	$q_{e(\text{exp})}$ (mg/g)	11.06	21.45	27.66	38.21
	$q_{e(\text{cal})}$ (mg/g)	0.47	8.00	1.70	0.40
	k_1 (1/min)	0.0001	0.0002	0.0002	0.0001
	R^2	0.704	0.971	0.881	0.847
AC	$q_{e(\text{exp})}$ (mg/g)	11.47	23.23	34.31	46.00
	$q_{e(\text{cal})}$ (mg/g)	0.14	0.25	0.27	0.16
	k_1 (1/min)	0.0001	0.0001	0.0001	0.0001
	R^2	0.856	0.864	0.945	0.681
OB	$q_{e(\text{exp})}$ (mg/g)	10.49	21.43	26.86	35.64
	$q_{e(\text{cal})}$ (mg/g)	7.21	1.71	2.48	1.15
	k_1 (1/min)	0.0002	0.0002	0.0002	0.0002
	R^2	0.882	0.764	0.967	0.871

Table 3. Kinetic parameters for the pseudo-second-order model.

Adsorbent	Parameter	C_0 (mg/L)			
		50	100	150	200
RH-550	$q_{e(\text{exp})}$ (mg/g)	7.70	17.97	25.70	35.70
	$q_{e(\text{cal})}$ (mg/g)	8.08	18.24	25.77	35.71
	k_2 (g/mg·min)	0.0171	0.0216	0.0660	0.245
	R^2	0.994	0.999	1	1
RH-700	$q_{e(\text{exp})}$ (mg/g)	11.38	18.15	25.26	35.41
	$q_{e(\text{cal})}$ (mg/g)	11.61	18.38	25.25	35.46
	k_2 (g/mg·min)	0.0293	0.0269	0.0550	0.2410
	R^2	0.997	0.999	0.999	1
WS-550	$q_{e(\text{exp})}$ (mg/g)	11.17	19.80	30.12	39.21
	$q_{e(\text{cal})}$ (mg/g)	11.20	19.92	30.21	39.22
	k_2 (g/mg·min)	0.1704	0.0579	0.0788	0.0844
	R^2	1	0.999	1	1
WS-700	$q_{e(\text{exp})}$ (mg/g)	11.06	21.45	27.66	38.21
	$q_{e(\text{cal})}$ (mg/g)	11.05	21.98	27.70	38.17
	k_2 (g/mg·min)	0.1587	0.0120	0.0654	0.2288
	R^2	1	0.999	1	1
AC	$q_{e(\text{exp})}$ (mg/g)	11.47	23.23	34.31	46.00
	$q_{e(\text{cal})}$ (mg/g)	11.47	23.26	34.25	46.08
	k_2 (g/mg·min)	0.5940	0.3243	0.2508	0.4709
	R^2	1	1	1	1
OB	$q_{e(\text{exp})}$ (mg/g)	10.49	21.43	26.86	35.64
	$q_{e(\text{cal})}$ (mg/g)	12.48	21.69	26.95	35.71
	k_2 (g/mg·min)	0.0030	0.0271	0.0470	0.0808
	R^2	0.934	0.999	1	1

values for the same concentrations were reported as 7.70, 17.97, 25.70, and 35.70 mg/g. The close agreement between $q_{e(\text{exp})}$ and $q_{e(\text{cal})}$ and the proximity of R^2 to 1 indicated that the pseudo-second-order kinetic model provided a better fit to the data than the pseudo-first-order kinetic model. This means that the SDS adsorption mechanism is predominantly via the process of chemisorption between adsorbate molecules (SDS) and specific adsorption sites on the adsorbent surface. This supports the explanation in Section 3.2, suggesting that hydrophobic interaction between SDS molecules and hydrophobic active sites on the adsorbent surface is potentially responsible for SDS removal [45,46]. From Table 3, it can also be observed that k_2 decreased as the initial concentration increased, particularly for adsorbents RH-550, RH-700, WS-700, and AC. It has been suggested that an increase in concentration increases competition between SDS molecules for available adsorption sites, as there is a finite number of active sites [49].

3.7.3. Intraparticle diffusion model

Weber and Morris's equation, also referred to as the intraparticle diffusion (IPD) model, is extensively utilised for describing diffusion-controlled adsorption processes. The linearised form of the model, represented by Equation (5), features q_t (mg/g) as the amount of SDS adsorbed (mg/g) onto the adsorbents at any time t (min), k_i as the intraparticle diffusion rate constant (g/mg min), and the intercept C as the boundary layer effect or surface adsorption [67]. A plot of q_t against $t^{0.5}$ was created for each investigated adsorbent, and a linear regression equation was derived through data fitting to determine the values of k_i and C . The determination coefficient (R^2) was calculated to assess the

suitability of the kinetic model for the experimental data.

$$q_t = k_i t^{0.5} + C \quad (5)$$

Fig. S6 illustrates the IPD kinetic plots alongside the R^2 values (supplementary information). Upon analysing the kinetic data using the IPD model, it was observed that the plot did not intersect the origin, indicating that IPD alone was not the sole rate-limiting step. This is consistent with the average R^2 values for each of the tested materials, which were not close to 1. Specifically, average R^2 values of 0.678, 0.493, 0.475, 0.646, 0.633, and 0.638 were found for RH-550, RH-700, WS-550, WS-700, AC, and OB, respectively. Furthermore, the intercept values (C), representing the impact of surface adsorption, increased with the rising concentration of the SDS solution, indicating an increase in the thickness of the boundary and a reduction in the likelihood of external mass transfer (Table 4). Higher intercept values, C , indicated a greater contribution of surface adsorption to the rate-limiting step [68]. This supports the findings of the pseudo-second-order model, suggesting that the SDS adsorption occurred when SDS molecules were bound to specific adsorption sites on the adsorbent surface.

3.8. Adsorption isotherms

Adsorption isotherms establish the relationship between the amount of adsorbate adsorbed by a unit weight of adsorbent and the concentration of adsorbate in the liquid phase at equilibrium and constant temperature [69]. Adsorption isotherms are useful for determining the nature of the adsorption process between an adsorbate and an adsorbent, such as monolayer chemical adsorption, multilayer physical adsorption, and ion exchange [70]. Furthermore, adsorption isotherm models provide information about adsorbent performance, such as maximum adsorption capacity [70]. Several isotherm models are commonly applied in adsorption systems, namely, the Langmuir model [71,72], the Freundlich model [73], the Sips model [74], the Temkin model [75], and the Brunauer–Emmett–Teller model [76]. In this study, the experimental results were interpreted according to Freundlich, Langmuir, and Temkin adsorption isotherms. The experimental results were primarily interpreted based on the first two models for comparative purposes with the existing literature on SDS adsorption (Table 5).

3.8.1. Langmuir isotherm model

The Langmuir isotherm assumes a fixed number of homogeneous active sites on the surface of any

Table 4. Kinetic parameters for the intraparticle diffusion model.

Adsorbent	Parameter	C_0 (mg/L)			
		50	100	150	200
RH-550	C	3.90	13.49	22.92	35.20
	k_i (g/mg·min ^{0.5})	0.3472	0.3942	0.2487	0.0390
	R^2	0.481	0.833	0.688	0.710
RH-700	C	7.57	12.93	24.45	34.61
	k_i (g/mg·min ^{0.5})	0.3535	0.4753	0.0529	0.0729
	R^2	0.362	0.656	0.538	0.415
WS-550	C	10.01	16.36	28.24	36.79
	k_i (g/mg·min ^{0.5})	0.1057	0.3195	0.1691	0.2222
	R^2	0.376	0.414	0.690	0.420
WS-700	C	10.28	13.70	25.61	37.47
	k_i (g/mg·min ^{0.5})	0.0645	0.6880	0.1804	0.0665
	R^2	0.430	0.783	0.707	0.665
AC	C	11.25	22.87	34.05	45.57
	k_i (g/mg·min ^{0.5})	0.0187	0.0306	0.0189	0.0382
	R^2	0.604	0.572	0.943	0.414
OB	C	2.63	15.64	23.82	34.76
	k_i (g/mg·min ^{0.5})	0.7023	0.5334	0.2730	0.0711
	R^2	0.672	0.520	0.614	0.744

adsorbent material, and saturation of these active sites prevents adsorbate adsorption. According to this model, the adsorption of adsorbate occurs until a monolayer of adsorption has been completed without further interaction between the adsorbent and adsorbate molecules [70,77]. The linearised form of the model can be expressed in Equation (5), where C_e (mg/L) is the equilibrium concentration, q_e (mg/g) is the amount of SDS adsorbed at equilibrium, q_{max} is the maximum adsorption capacity (mg/g), and K_L is the equilibrium Langmuir constant. Based on the slope ($1/q_{max}$) and intercept ($1/(q_{max}K_L)$) for the linear fitting of the plot of C_e/q_e versus C_e , the model parameters q_{max} and K_L were evaluated. Values of R^2 were calculated to determine the suitability of the isotherm model for the experimental data.

$$C_e/q_e = (1/q_{max})C_e + 1/q_{max}K_L \quad (5)$$

Figure 8a shows the plot of the Langmuir isotherm model for each of the adsorbents evaluated in this study. Based on the plot, model parameters are shown in Table 5. The average R^2 values of 0.607, 0.761, 0.735, 0.925, 0.963, and 0.955 were reported for RH-550, RH-700, WS-550, WS-700, AC, and OB, respectively. Overall, the experimental data on SDS adsorption using the adsorbents RH-550, RH-700, and WS-550 (R^2 value < 0.90) did not fit the Langmuir model, unlike WS-700, AC, and OB. In the literature, the use of the Langmuir model to fit experimental data on the adsorption of anionic surfactants (e.g. SDS and SDBS) has also been reported when using carbon black [78], activated coconut shell [49], chitosan hydrogel beads [79], and almond shell activated carbon [60] (Table 5). Additionally, according to Table 5, an increase in the initial concentration (mg/L) led to an increase in the SDS equilibrium adsorption capacity. This can be explained because higher loadings result in a greater driving force [49,56].

Table 5. Parameters for the Langmuir, Freundlich and Temkin isotherms models.

	Adsorbent					
	RH-550	RH-700	WS-550	WS-700	AC	OB
<i>Langmuir</i>						
q_{max} (mg/g)	49.75	43.67	66.23	42.74	80.65	45.87
K_L (L/mg)	0.02	0.04	0.03	0.07	0.13	0.05
R^2	0.607	0.761	0.735	0.925	0.963	0.955
<i>Freundlich</i>						
K_F (mg/g)	3.27	5.09	3.67	7.22	10.63	4.75
n	1.86	2.31	1.59	2.56	1.51	2.01
R^2	0.879	0.903	0.919	0.978	0.959	0.953
<i>Temkin</i>						
K_T (L/g)	0.30	0.56	0.36	1.09	1.42	0.47
b (J/mol)	10.22	8.49	13.49	8.15	17.26	10.30
R^2	0.739	0.783	0.867	0.902	0.994	0.958

3.8.2. Freundlich isotherm model

According to the Freundlich isotherm theory, adsorbate binds to heterogeneous surfaces with different types of sites acting simultaneously, each with its free energy of sorption [80]. Thus, in contrast to the Langmuir isotherm, this model can be used to analyse multilayer adsorption on heterogeneous sites. The linear form of the Freundlich isotherm is expressed in Equation (6), where q_e (mg/g) is the amount of SDS adsorbed at equilibrium, K_F (mg/g) is the adsorption capacity, n is a constant representing affinity and favourability of adsorption, and C_e (mg/L) is the equilibrium concentration. The values of K_F and n were estimated from the slope and intercept, respectively, of a plot of $\ln q_e$ against $\ln C_e$. R^2 values were calculated to determine the suitability of the isotherm model.

$$\ln q_e = \ln K_F + (1/n) \ln C_e \quad (6)$$

Figure 8b shows the Freundlich isotherm model for each of the adsorbents evaluated in this study. Freundlich model parameters are described in Table 5. The average R^2 values for RH-550, RH-700, WS-550, WS-700, AC, and OB were 0.879, 0.903, 0.919, 0.978, 0.959, and 0.953, respectively. Unlike the Langmuir model, the experimental data on SDS adsorption using the adsorbents RH-700, WS-550, and WS-700 fitted better to the Freundlich. In the case of adsorbents AC and OB, the R^2 values are similar for both Langmuir and Freundlich models, suggesting that experimental data on SDS adsorption using both adsorbents well-fitted with both isotherm models. Experimental data concerning anionic surfactant adsorption in the literature has also been found to fit the Freundlich isotherm model (Table 5). For instance, Purakayastha et al. [40] demonstrated that the Freundlich model provided a better data fit for SDS adsorption with waste rubber granules, wood charcoal, and silica gel. A similar isotherm model fitting was reported by Kyzas et al. [81] and Sen et al. [47] when using akaganeite and pine cone biomass, respectively. Concerning the favourability of the adsorption process, Huang et al. [82] stated that the adsorption process is favourable, moderately difficult, and poor for n values of 2 - 10, 1 - 2, and less than 1, respectively. Based on the results obtained, it appears the adsorption process was favourable for RH-700, WS-700, and AC; while moderately difficult for the rest of the adsorbents (Table 5).

3.8.3. Temkin isotherm model

The Temkin isotherm model postulates that the adsorption heat of all molecules decreases linearly

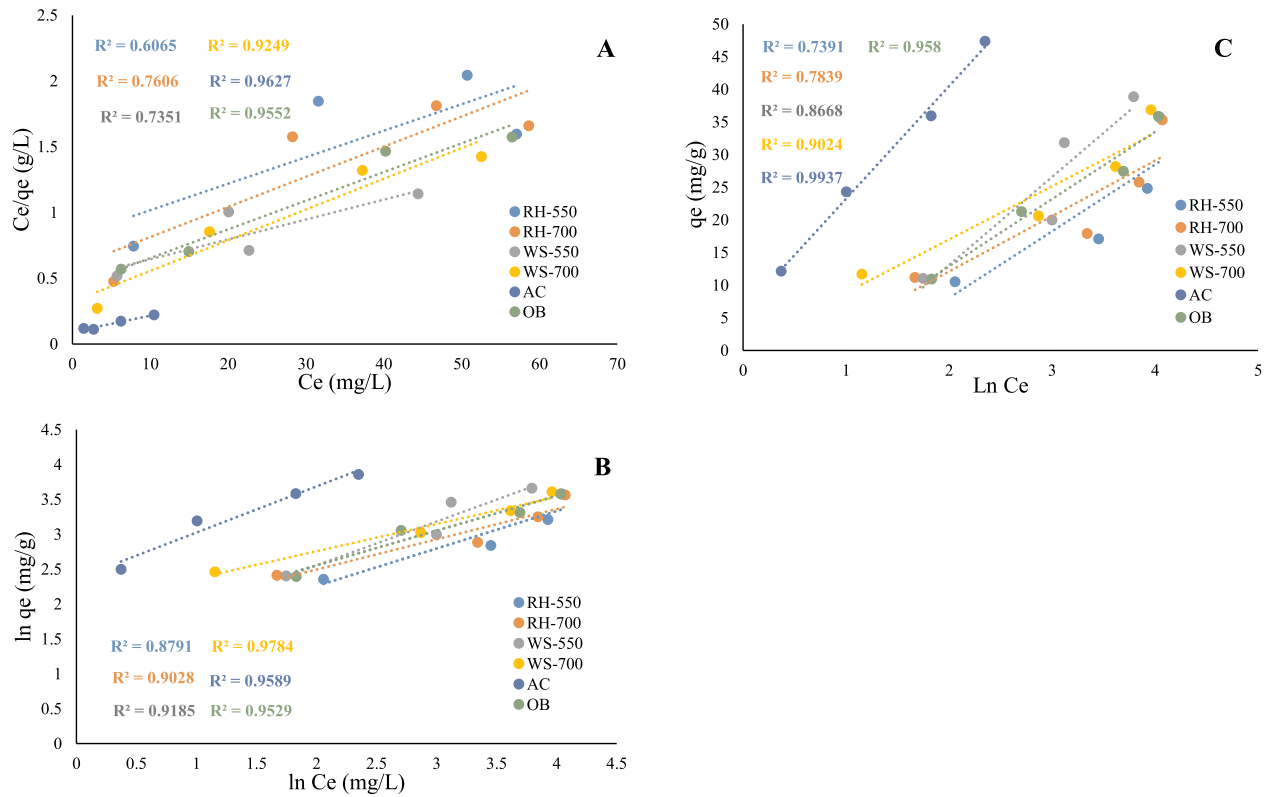


Figure 8. Adsorption isotherms plots: A) Langmuir isotherm; B) Freundlich isotherm; C) Temkin isotherm.

with the increase in the coverage of the adsorbent surface. The linear form of the Temkin isotherm can be represented in Equation (7), where K_T (L/mg) is the Temkin isotherm constant, b (J/mol) is the Temkin constant associated with the heat of sorption, R is the universal gas constant (8.314 J/mol·K), and T is the temperature (K). Positive and negative values of b indicate that the adsorption process is exothermic and endothermic, respectively [83]. The values of K_T and b were estimated from the intercept and slope, respectively, of a plot of q_e (mg/g) against $\ln C_e$. R^2 values were calculated to determine the suitability of the isotherm model. The Temkin constant, b (J/mol), was 10.22, 8.49, 13.49, 8.15, 17.26, and 10.30 J/mol for RH-550, RH-700, WS-550, WS-700, AC, and OB, respectively (Table 5). This suggested that the SDS adsorption process was exothermic. Such behaviour occurs because, upon adsorption of the adsorbate (SDS molecules) onto the surface of the adsorbents, there is a reduction in the energy of the adsorbent, resulting in the release of heat [84]. Moreover, the Temkin isotherm achieved a good fit for the SDS adsorption data with R^2 values above 0.9 only for WS-700 (0.902), AC (0.994), and OB (0.958).

$$q_e = (R_t/b)\ln K_T + (R_t/b)\ln C_e \quad (7)$$

3.9. Possible SDS removal mechanism

According to Kalam et al. [85], surfactant adsorption isotherms exhibit the Somasundaran-Fuerstenau shape and are consequently divided into four regions. In Region I, adsorption occurs due to the electrostatic attraction between the charged surface and surfactant ions. In Region II, electrostatic interactions and lateral hydrophobic interactions between hydrocarbon chains (hydrophobic tail) result in surfactant aggregates forming hemimicelles and admicelles. In Region III, surfactant adsorption neutralises the adsorbent surface, causing the adsorption driving force to shift to lateral hydrophobic interactions. In Region IV, the plateau region of surfactant adsorption occurs, and lateral hydrophobic interactions become the primary driving force, leading to the formation of surfactant aggregates in the shape of micelles (Figure 9). In this study, the dominant mechanism responsible for SDS adsorption appears to be the electrostatic attraction between the hydrophilic head of the surfactant and the negatively charged biochar surface, along with the hydrophobic interactions between the hydrophobic tails of surfactant molecules. Additionally, the presence of hydrophobic sites on the biochar surface, it is believed that the hydrophobic tails of surfactant molecules are forced to associate with the biochar hydrophobic surfaces by entropic

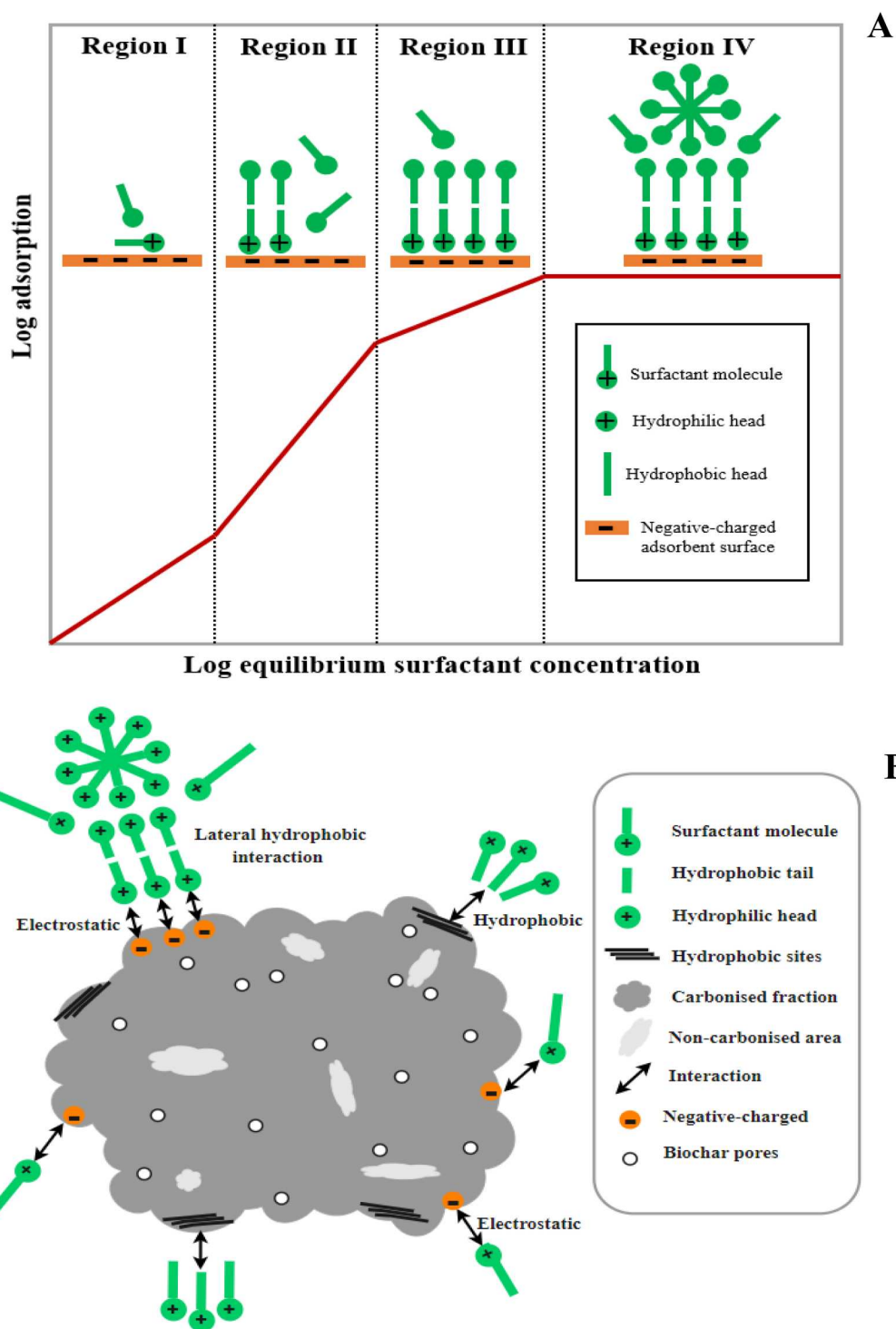


Figure 9. Scheme of common surfactant adsorption isotherm (A). Surfactant adsorption mechanism (B). Adapted from Kalam et al. [85] and Inyang & Dickenson [86].

and enthalpic favourability [87]. Figure 9 illustrates the common surfactant adsorption isotherm and a hypothetical adsorption mechanism on the biochar surface.

The surface chemistry of the adsorbents under study also provided insights into the possible SDS removal mechanisms. Figure 10 shows the FTIR spectra of the

biochar adsorbent and AC materials before and after SDS adsorption. Prior to SDS adsorption, the adsorbents exhibited oxygen-containing functional groups, crucial in the removal of anionic surfactants [31]. For instance, the adsorbent materials showed hydroxyl (–O–H) stretching vibrations groups and carbonyl (C = O) stretching of

as akaganeite [81], almond shell activated carbon [60], multiwalled carbon nanotubes [58], activated carbon with bacteria [90], and carbide-derived carbon [57], the maximum adsorption capacity for each biochar was found to be lower. This can be explained by the fact that used biochars have a much smaller total surface area than the last-mentioned adsorbents. For instance, the average surface area for RH-550, RH-700, WS-550, and WS-700, was 20.10, 42, 26.40, and 23.20 m²/g, respectively; whereas the surface area of akaganeite, almond shell activated carbon, carbon nanotubes, activated carbon with bacteria, and carbide-derived carbon was 330, 1600, 233, 1400, and 1120 m²/g, respectively. Thus, as adsorption is proportional to the surface area, adsorbents with a high surface area have more adsorption sites, resulting in a higher adsorption capacity [17]. It is worth mentioning that there are not many studies evaluating the use of biochar to remove anionic surfactants. Despite this, overall biochars appear to offer excellent potential for removing SDS.

3.11. Potential application

This study assessed the efficacy of biochar adsorbents in removing the anionic surfactant SDS from an aqueous

solution, comparing their performance to conventional AC. The findings highlight the potential of biochar, derived from the pyrolysis of agricultural and forestry waste, to be a cost-effective and bio-based adsorbent for the removal of anionic surfactant in real wastewater. As a type of wastewater, greywater from hand basins, bath/showers, kitchens, and laundry, typically contains high concentrations of anionic surfactants. For instance, Shreya et al. [11] reported anionic surfactant concentrations of 42 - 118.3, 14.9–61, 59 and 41.9 mg/L in laundry, shower, kitchen, and washbasin greywater, respectively. In light of the pressing need for affordable and sustainable greywater treatment methods, especially in resource-poor environments, utilising biochar as a filter medium in technologies targeting anionic surfactant removal presents an effective strategy to enhance greywater quality for various water reuse purposes (e.g. cleaning, toilet flushing, and crop irrigation) [12,13]. Biochar could serve as an alternative adsorbent material to AC or sand in standard column filtration systems for greywater treatment. Moreover, employing biochar derived from biomass waste facilitates the adoption of biochar-based greywater treatment technologies in low- and middle-income countries with abundant agricultural (e.g. rice husk and wheat straw) and forestry waste (e.g.

Table 6. Comparison of SDS adsorption by various adsorbents.

Anionic surfactant	Adsorbent	Surface area (m ² /g)	Isotherm	Studied concentration (mg/L)	Maximum adsorption capacity (mg/g)	Reference
SDS	RH-550	20.10	Freundlich	50–200	49.75	This study
SDS	RH-700	42	Freundlich	50–200	43.67	This study
SDS	WS-550	26.40	Freundlich	50–200	66.23	This study
SDS	WS-700	23.20	Freundlich	50–200	42.74	This study
SDS	AC	1500–3000	FreundlichLangmuir	50–200	80.65	This study
SDS	OB	300	Freundlich Langmuir	50–200	45.87	This study
SDS	Fishscale	–	–	100	51.55	[48]
SDS	Seashell	–	–	100	49.80	[48]
SDS	Akaganeite	330	Freundlich Langmuir	–	823.96	[81]
SDS	Paper fiber	1.5	Langmuir	–	0.30	[78]
SDS	Carbon black	96	Langmuir	–	55.68	[78]
SDS	Activated coconut shell	674	Langmuir	80–280	111.1	[49]
SDS	Chitosan hydrogel beads	–	Langmuir	10–60	76.9	[79]
SDS	Aquaguard waste activated carbon	1250	Langmuir	15	61.35	[53]
SDS	Granular activated carbon	–	Freundlich Langmuir	2	3.75	[40]
SDS	Waste tyre rubber granule	0.45–0.78	Freundlich Langmuir	2	4.16	[40]
SDS	Wood charcoal	–	Freundlich	2	5.17	[40]
SDS	Silica gel	–	Freundlich	2.0	5.18	[40]
SDS	Pinecone biomass	0.213	Freundlich Langmuir	10–80	95.75	[47]
SDS	Standard activated carbon	–	Langmuir	–	117.2	[89]
SDS	Ammonium chloride-induced pomegranate wood waste	–	Langmuir	–	178.6	[89]
SDBS	Carbon black	105	–	3.8–768.9	175	[57]
SDBS	Carbide derived carbon	1120	Sips	139.4–697	442	[57]
SDBS	MultiWalled Carbon Nanotubes	233	Brouers-Sotolongo	5–150	313	[58]
SDBS	Activated carbon	1201	Redlich-Peterson	10–125	146	[59]
SDBS	Activated carbon with bacteria	1400	–	250	158	[90]
SDBS	Almond shell activated carbon	1600	Langmuir	250	468.8	[60]

wood residues). For instance, biochar can be integrated into nature-based solutions such as constructed wetlands, green walls, vertical gardens, and green roofs, which are commonly low-cost and sustainable greywater treatment techniques in developing countries [19]. Therefore, employing biochar as an adsorbent material for greywater treatment, specifically targeting anionic surfactant removal, can be viewed as a synergistic strategy promoting the circular economy in both the wastewater and agricultural and forestry waste sectors [16].

3.12. Future research

This study focused on examining the SDS removal potential of five types of biochar and determining the operational conditions (pH, adsorbent loading, adsorbent size, contact time, and initial concentration) to optimise SDS removal at room temperature. Thus, the findings of SDS removal in our study are limited to this temperature condition. Further research is still necessary to improve the efficiency of the SDS removal process to allow scaling-up initiatives. Future studies should focus on identifying the optimum pre-treatment processes to increase the surface area of biochars, aiming to enhance the adsorption capacity to a level comparable to commercial adsorbent products. Furthermore, a comprehensive study of the SDS removal mechanism should be conducted to identify possible modifications to the biochar surface that enhance its ability to bind SDS. Additionally, further investigations should evaluate the use of biochar-based filtration systems to remove anionic surfactants from real greywater (e.g. wastewater from handwashing, laundry, kitchen, and bathroom activities). This can help understand the effect of the greywater matrix on the SDS removal efficiency and gain insights into the efficacy of biochar-based filtration systems as a decentralised greywater treatment process. Furthermore, upcoming studies should conduct a thorough investigation into the regeneration of wheat straw biochar produced at 550°C (WS-550), which demonstrated the highest SDS adsorption capacity (66.2 mg/g) when compared to other biochars examined. Also, further research is needed to focus on understanding leachability of potential contaminants (e.g. heavy metals), that might be present in biochars. Additional research is required to explore various regeneration techniques (e.g. thermal, chemical) for used biochars, aiming to potential reuse biochars for sustainable wastewater treatment.

4. Conclusion

This study demonstrated that biochar derived from agricultural and forestry residues is an effective adsorbent for anionic surfactants in aqueous solutions. Various

operational factors, including pH, adsorbent loading, adsorbent size, contact time, and initial concentration, were found to influence SDS removal. The removal of SDS at different pH levels was similar for biochars, indicating that hydrophobic interactions are the main cause of adsorption. Increased dosages of adsorbent also increased SDS uptake; however, dosages exceeding 6 g/L result in decreased adsorption. The increased particle size of the adsorbent reduced the surface area, thereby decreasing SDS removal. Biochars demonstrated the ability to adsorb half of the SDS within 10 min, suggesting a large number of adsorption sites on the surface. SDS removal decreased as the initial concentration increased, except for AC, suggesting that surface area is the major limiting factor. Under optimised operating conditions, the maximum extent of removal was 78%, 82.4%, 89.5%, 90.4%, 97%, and 88.4% for adsorbents RH-550, RH-700, WS-550, WS-700, AC, and OB, respectively. The maximum adsorption capacity was reported in the range of 42.7 - 66.2 and 80.6 mg/g for biochars and AC, respectively. WS-550 achieved an adsorption capacity comparable to carbon black and commercial Aquaguard waste-activated carbon, offering a sustainable and low-cost alternative to those materials. SDS adsorption appears to be the primary chemisorption process, as indicated by the kinetic data fitting well into the pseudo-second-order kinetic model. The Freundlich isotherm model exhibited a better fit for the experimental data on SDS adsorption using all tested adsorbents except for RH-550. However, both the Langmuir and Freundlich models demonstrated a better fit for the experimental data on SDS adsorption using WS-700, AC, and OB. Overall biochars are promising adsorbents with a high potential for removing SDS from aqueous solutions.

Acknowledgements

We would like to acknowledge the Centre for Agroecology, Water, and Resilience at Coventry University (UK) for the graduate scholarship grant (Project Code 13911-06). We want to acknowledge the UK Biochar Research Centre for providing biochar samples. We wish to acknowledge Sam Towers and Richard Collins for their technical assistance in conducting the experiments. We also want to acknowledge Prof. Sue Charlesworth for her valuable feedback on the manuscript.

Disclosure statement

No potential conflict of interest was reported by the author(s).

Credit authorship contribution statement

Jhonny Ismael Bautista Quispe: Conceptualisation, Methodology, Data collection, Data visualisation,

Artwork, Writing – original draft. **Anna Bogush:** Supervision, Conceptualisation, Funding, Resources, Data collection, Writing, Review & editing. **Luiza C. Campos:** Supervision, Review & editing. **Ondrej Masek:** Supervision, Review & editing, Resources (biochar).

Declaration of competing interest

There are no competing financial interests or personal relationships that may have influenced the work reported in this paper by the authors.

Data availability

A reasonable request should be made to the corresponding author for access to the data.

ORCID

L. C. Campos  <http://orcid.org/0000-0002-2714-7358>

References

- [1] Pinazo A, Pérez L, del Carmen Morán M^a, et al. Arginine-based surfactants: synthesis, aggregation properties, and applications. In: DG Hayes, DKY Solaiman, RD Ashby, editors. *Biobased surfactants*. Amsterdam: Elsevier; 2019. p. 413–455. doi:10.1016/B978-0-12-812705-6.00013-7
- [2] Aboulhassan MA, Souabi S, Yaacoubi A, et al. Removal of surfactant from industrial wastewaters by coagulation flocculation process. *Int J Environ: Sci Technol*. 2006;3:327–332. doi:10.1007/BF03325941
- [3] Gao Q, Chen W, Chen Y, et al. Surfactant removal with multiwalled carbon nanotubes. *Water Res*. 2016;106:531–538. doi:10.1016/j.watres.2016.10.027
- [4] Olkowska E, Ruman M, Polkowska Ż. Occurrence of surface active agents in the environment. *J Anal Methods Chem*. 2014;2014:1–15. doi:10.1155/2014/769708
- [5] St. Laurent JB, de Buzzaccarini F, De Clerck K, et al. Laundry cleaning of textiles. In: I Johansson, P Somasundaran, editors. *Handbook for cleaning/decontamination of surfaces*. Amsterdam: Elsevier; 2007. p. 57–102. doi:10.1016/B978-0-44451664-0/50003-6
- [6] Pettersson A, Adamsson M, Dave G. Toxicity and detoxification of Swedish detergents and softener products. *Chemosphere*. 2000;41(10):1611–1620. PMID: 11057688. doi:10.1016/S0045-6535(00)00035-7
- [7] Ramcharan T, Bissessur A. Analysis of linear alkylbenzene sulfonate in laundry wastewater by HPLC–UV and UV–Vis spectrophotometry. *J Surfact Deterg*. 2016;19:209–218. doi:10.1007/s11743-015-1763-x
- [8] Badmus SO, Amusa HK, Oyehan TA, et al. Environmental risks and toxicity of surfactants: overview of analysis, assessment, and remediation techniques. *Environ Sci Pollut Res*. 2021;28:62085–62104. doi:10.1007/s11356-021-16483-w
- [9] Effendi I, Nedi S, Pakpahan R. Detergent disposal into our environment and its impact on marine microbes. *IOP Pragma Conf Ser: Earth Environ Sci*. 2017;97:012030. doi:10.1088/1755-1315/97/1/012030
- [10] Collivignarelli MC, Miino MC, Baldi M, et al. Removal of non-ionic and anionic surfactants from real laundry wastewater by means of a full-scale treatment system. *Process Saf Environ Prot*. 2019;132:105–115. doi:10.1016/j.psep.2019.10.022
- [11] Verma AK, Dash AK, Bhunia P, et al. Removal of surfactants in greywater using low-cost natural adsorbents: a review. *Surf Interfaces*. 2021;27:101532. doi:10.1016/j.surfin.2021.101532
- [12] Al-Jayyousi OR. Greywater reuse: towards sustainable water management. *Desalination*. 2003;156(1–3):181–192. doi:10.1016/S0011-9164(03)00340-0
- [13] Madungwe E, Sakuringwa S. Greywater reuse: A strategy for water demand management in Harare? *Phys Chem Earth, Parts A/B/C*. 2007;32(15–18):1231–1236. doi:10.1016/j.pce.2007.07.015
- [14] Boano F, Caruso A, Costamagna E, et al. A review of nature-based solutions for greywater treatment: applications, hydraulic design, and environmental benefits. *Sci Total Environ*. 2020;711:134731. doi:10.1016/j.scitotenv.2019.134731
- [15] Padrón-Páez JI, De-León Almaraz S, Román-Martínez A. Sustainable wastewater treatment plants design through multiobjective optimization. *Comput Chem Eng*. 2020;140:106850. doi:10.1016/j.compchemeng.2020.106850
- [16] Hossain N, Bhuiyan MA, Pramanik BK, et al. Waste materials for wastewater treatment and waste adsorbents for biofuel and cement supplement applications: A critical review. *J Clean Prod*. 2020;255:120261. doi:10.1016/j.jclepro.2020.120261
- [17] Enaime G, Baçaoui A, Yaacoubi A, et al. Biochar for wastewater treatment—Conversion technologies and applications. *Appl Sci*. 2020;10(10):3492. doi:10.3390/app10103492
- [18] Ennis CJ, Evans AG, Islam M, et al. Biochar: carbon sequestration, land remediation, and impacts on soil microbiology. *Crit Rev Environ Sci Technol*. 2012;42(22):2311–2364. doi:10.1080/10643389.2011.574115
- [19] Bautista Quispe JI, Campos LC, Mašek O, et al. Use of biochar-based column filtration systems for greywater treatment: A systematic literature review. *J Water Process Eng*. 2022;48:102908. doi:10.1016/j.jwpe.2022.102908
- [20] Babar AA, Memon SA, Ali MF, et al. Comparison of combined filter and activated carbon on treatment of synthetic greywater by produced mgcl₂ based activated carbon from rice straw waste. *Int J Agric Environ Biores*. 2019;4(4):107–120. doi:10.35410/IJAEB.2019.4412
- [21] Miles T, Rasmussen E, Gray M. Aqueous contaminant removal and stormwater treatment using biochar. In: M Guo, Z He, SM Uchimiya, editors. *Agricultural and environmental applications of biochar: advances and barriers*. Wisconsin: Soil Science Society of America, Inc.; 2015. p. 341–376. doi:10.2136/sssaspecpub63.2014.0048.5
- [22] Pokharel A. Application of biochar for efficient municipal wastewater treatment, Msc diss., University of Prince Edward Island, Charlottetown, 2020. <https://www.>

- islandscholar.ca/islandora/object/ir%3A23556/datastream/PDF/download Google Scholar.
- [23] Mandal A, Singh N. Optimization of atrazine and imidacloprid removal from water using biochars: designing single or multi-staged batch adsorption systems. *Int J Hyg: Environ Health*. 2017;220(3):637–645. doi:10.1016/j.ijheh.2017.02.010
- [24] Hussain A, Maitra J, Khan KA. Development of biochar and chitosan blend for heavy metals uptake from synthetic and industrial wastewater. *Appl Water Sci*. 2017;7:4525–4537. doi:10.1007/s13201-017-0604-7
- [25] Mašek O, Buss W, Roy-Poirier A, et al. Consistency of biochar properties over time and production scales: A characterisation of standard materials. *J Anal Appl Pyrolysis*. 2018;132:200–210. doi:10.1016/j.jaap.2018.02.020
- [26] Oxford Biochar Ltd. From one product we create many, 2020. Available online at: <https://www.oxfordbiochar.org/from-one-product-we-create-many/#:~:text=Biochar%20isn't%20a%20fertiliser,sustainable%20and%20durable%20soil%20improver> [accessed 2022 August 12].
- [27] Kim S, Dale BE. Global potential bioethanol production from wasted crops and crop residues. *Biomass Bioenerg*. 2004;26:361–375. doi:10.1016/j.biombioe.2003.08.002
- [28] Thengane SK, Kung K, Hunt J, et al. Market prospects for biochar production and application in California, biofuels. *Bioprod Bioref*. 2021;15(6):1802–1819. doi:10.1002/bbb.2280
- [29] Álvarez C, Mullen AM, Pojić M, et al. Chapter 2 - Classification and target compounds. In: CM Galanakis, editor. *Food waste recovery (second edition): processing technologies, industrial techniques, and applications*. Amsterdam: Elsevier; 2021. p. 21–49. doi:10.1016/B978-0-12-820563-1.00024-X
- [30] Ayranci E, Duman O. Removal of anionic surfactants from aqueous solutions by adsorption onto high area activated carbon cloth studied by in situ UV spectroscopy. *J Hazard Mater*. 2007;148(1–2):75–82. doi:10.1016/j.jhazmat.2007.02.006
- [31] Wu SH, Pendleton P. Adsorption of anionic surfactant by activated carbon: effect of surface chemistry, ionic strength, and hydrophobicity. *J Colloid Interface Sci*. 2001;243(2):306–315. doi:10.1006/jcis.2001.7905
- [32] Maziarka P, Wurzer C, Arauzo PJ, et al. Do you BET on routine? The reliability of N₂ physisorption for the quantitative assessment of biochar's surface area. *Chem Eng J*. 2021;418:129234. doi:10.1016/j.cej.2021.129234
- [33] Zhao JJ, Shen XJ, Domene X, et al. Comparison of biochars derived from different types of feedstock and their potential for heavy metal removal in multiple-metal solutions. *Sci Rep*. 2019;9:9869. doi:10.1038/s41598-019-46234-4
- [34] Janu R, Mrlik V, Ribitsch D, et al. Biochar surface functional groups as affected by biomass feedstock, biochar composition and pyrolysis temperature. *Carbon Resour Convers*. 2021;4:36–46. doi:10.1016/j.crcon.2021.01.003
- [35] Li B, Liu D, Lin D, et al. Changes in biochar functional groups and its reactivity after volatile–Char interactions during biomass pyrolysis. *Energy Fuels*. 2020;34(11):14291–14299. doi:10.1021/acs.energyfuels.0c03243
- [36] Collett C, Mašek O, Razali N, et al. Influence of biochar composition and source material on catalytic performance: The carboxylation of glycerol with CO₂ as a case study. *Catalysts*. 2020;10(9):1067. doi:10.3390/catal10091067
- [37] Guilhen SN, Watanabe T, Silva TT, et al. Role of point of zero charge in the adsorption of cationic textile dye on standard biochars from aqueous solutions: selection criteria and performance assessment. *Recent Progre Mate*. 2022;4(2):010. doi:10.21926/rpm.2202010
- [38] Jamrah A, Al-Futaisi A, Prathapar S, et al. Evaluating grey-water reuse potential for sustainable water resources management in Oman. *Environ Monit Assess*. 2008;137(1–3):315–327. doi:10.1007/s10661-007-9767-2
- [39] Adak A, Pal A, Bandyopadhyay M. Spectrophotometric determination of anionic surfactants in wastewater using acridine orange. *Indian J Chem Technol*. 2005;12:145–148. <http://nopr.niscpr.res.in/bitstream/123456789/8625/1/IJCT%2012%282%29%20145-148.pdf>.
- [40] Purakayastha PD, Pal A, Bandyopadhyay M. Adsorbent selection for anionic surfactant removal from water. *Indian J Chem Technol*. 2005;12:281–284. <https://nopr.niscpr.res.in/bitstream/123456789/8645/1/IJCT%2012%283%29%20281-284.pdf>.
- [41] UK Biochar Research Centre. UKBRC Standard Biochar, 2022. Available at: https://www.biochar.ac.uk/standard_materials.php (accessed 2022 August 11).
- [42] Elnour AY, Alghyamah AA, Shaikh HM, et al. Effect of pyrolysis temperature on biochar microstructural evolution, physicochemical characteristics, and its influence on biochar/polypropylene composites. *Appl Sci*. 2019;9(6):1149. doi:10.3390/app9061149
- [43] Pavan PC, Crepaldi EL, Valim JB. Sorption of anionic surfactants on layered double hydroxides. *J Colloid Interface Sci*. 2000;229(2):346–352. doi:10.1006/jcis.2000.7031
- [44] Nowrouzi I, Mohammadi AH, Manshad AK. Preliminary evaluation of a natural surfactant extracted from *Myrtus communis* plant for enhancing oil recovery from carbonate oil reservoirs. *J Petrol Explor Prod Technol*. 2022;12:783–792. doi:10.1007/s13202-021-01336-6
- [45] Bindaes MMM, Franco MR. Surfactant removal from aqueous solutions onto activated carbon using UV spectroscopy. *Desalin Water Treat*. 2015;56(11):2890–2895. doi:10.1080/19443994.2014.963157
- [46] Schouten N, van der Ham LGJ, Euverink G-JW, et al. Selection and evaluation of adsorbents for the removal of anionic surfactants from laundry rinsing water. *Water Res*. 2007;41(18):4233–4241. doi:10.1016/j.watres.2007.05.044
- [47] Sen TK, Thi MT, Afroze S, et al. Removal of anionic surfactant sodium dodecyl sulphate from aqueous solution by adsorption onto pine cone biomass of *Pinus Radiate*: equilibrium, thermodynamic, kinetics, mechanism and process design. *Desalination Water Treat*. 2012;45(1–3):263–275. doi:10.5004/dwt.2012.3331
- [48] Than MM, Aung NN, Zin AT. Study on sorption properties of activated biosorbents (fishscale and seashell) for the removal of anionic surfactant. *J Myanmar Acad Arts Sci*. 2020;18(1A):77–88. [http://maas.edu.mm/Research/Admin/pdf/7.%20Daw%20Myint%20Myint%20Than\(77-88\).pdf](http://maas.edu.mm/Research/Admin/pdf/7.%20Daw%20Myint%20Myint%20Than(77-88).pdf).

- [49] Bhandari PS, Gogate PR. Kinetic and thermodynamic study of adsorptive removal of sodium dodecyl benzene sulfonate using adsorbent based on thermochemical activation of coconut shell. *J Mol Liq.* 2018;252:495–505. doi:10.1016/j.molliq.2017.12.018
- [50] Mi-Na Z, Xue-Pin L, Bi S. Adsorption of surfactants on chromium leather waste. *J Soc Leather Technol Chem.* 2006;90(1):1–6. <https://citeseerx.ist.psu.edu/document?repid=rep1&type=pdf&doi=efbdae493f2994a0a2792ba1f7e9ab90b264f4d4>.
- [51] Ersa NS, Ikhwali MF, Karunia TU. Adsorption mechanism on surfactant removal using eggshell waste and rice straw as economically biosorbent. *IOP Conf Ser: Earth Environ Sci.* 2021;871:012034. doi:10.1088/1755-1315/871/1/012034
- [52] Veli S, Arslan A, Topkaya E, et al. Investigation of grey-water treatment by adsorption process using polymeric composites supported with activated carbon. *Eurasian J Environ Res.* 2018;2(2):14–20. <https://dergipark.org.tr/en/pub/ejere/issue/39128/426771>.
- [53] Gupta S, Pal A, Ghosh PK, et al. Performance of waste activated carbon as a low-cost adsorbent for the removal of anionic surfactant from aquatic environment. *J Environ Sci Health, Part A.* 2003;38(2):381–397. doi:10.1081/ESE-120016902
- [54] Purakayastha PD, Pal A, Bandyopadhyay M. Adsorption of anionic surfactant by a low-cost adsorbent. *J Environ Sci Health, Part A.* 2002;37(5):925–938. doi:10.1081/ESE-120003598
- [55] Chatterjee R, Sajjadi B, Chen W-Y, et al. Effect of pyrolysis temperature on physicochemical properties and acoustic-based amination of biochar for efficient CO₂ adsorption. *Front Energy Res.* 2020;8:1–18. doi:10.3389/fenrg.2020.00085
- [56] Ahmad R, Kumar R. Adsorptive removal of Congo red dye from aqueous solution using bael shell carbon. *Appl Surf Sci.* 2010;257(5):1628–1633. doi:10.1016/j.apsusc.2010.08.111
- [57] Kochkodan O, Maksin V. Mixed adsorption of cetyltrimethylammonium bromide and Triton X-100 surfactants on carbon black. *J Serbian Chem Soc.* 2018;936:8–18. doi:10.4028/www.scientific.net/msf.936.8
- [58] Ncibi MC, Gaspard S, Sillanpää M. As-synthesized multi-walled carbon nanotubes for the removal of anionic and nonionic surfactants. *J Hazard Mater.* 2015;286:195–203. doi:10.1016/j.jhazmat.2014.12.039
- [59] Valizadeh S, Younesi H, Bahramifar N. Highly mesoporous K₂CO₃ and KOH-activated carbon for SDBS removal from water samples: batch and fixed-bed column adsorption process, environ. nanotechnology. *Monit Manag.* 2016;6:1–13. doi:10.1016/j.enmm.2016.06.005
- [60] Bautista-Toledo MI, Rivera-Utrilla J, Méndez-Díaz JD, et al. Removal of the surfactant sodium dodecylbenzenesulfonate from water by processes based on adsorption/bioadsorption and biodegradation. *J Colloid Interface Sci.* 2014;418:113–119. doi:10.1016/j.jcis.2013.12.001
- [61] Ossman ME, Mansour MS. Removal of Cd(II) ion from wastewater by adsorption onto treated old newspaper: kinetic modeling and isotherm studies. *Int J Ind Chem.* 2013;4:13. doi:10.1186/2228-5547-4-13
- [62] Barka N, Abdennouri M, Makhfouk ME, et al. Biosorption characteristics of cadmium and lead onto eco-friendly dried cactus (*Opuntia ficus indica*) cladodes. *J Environ Chem Eng.* 2013;1(3):144–149. doi:10.1016/j.jece.2013.04.008
- [63] Suganya E, Rangabhashiyam S, Lity AV, et al. Removal of hexavalent chromium from aqueous solution by a novel biosorbent *Caryota urens* seeds: equilibrium and kinetic studies. *Desalination and Water Treat.* 2016;57(50):23940–23950. doi:10.1080/19443994.2015.1134355
- [64] Cotoruelo LM, Marqués MD, Rodríguez-Mirasol J, et al. Lignin-based activated carbons for adsorption of sodium dodecyl benzene sulfonate: equilibrium and kinetic studies. *J Colloid Interface Sci.* 2009;332(1):39–45. doi:10.1016/j.jcis.2008.12.031
- [65] Sahoo TR, Prelot B. Chapter 7 - adsorption processes for the removal of contaminants from wastewater: the perspective role of nanomaterials and nanotechnology. In: B Bonelli, FS Freyria, I Rosetti, R Sethi, editors. *Nanomaterials for the detection and removal of wastewater pollutants*. Amsterdam: Elsevier; 2020. p. 161–222. doi:10.1016/B978-0-12-818489-9.00007-4
- [66] Lagergren S. About the theory of so-called adsorption of soluble substances. *Kungliga Svenska Vetenskapsakademiens Handlingar.* 1898;24:1–39.
- [67] Pholosi A, Naidoo EB, Ofomaja AE. Intraparticle diffusion of Cr(VI) through biomass and magnetite coated biomass: A comparative kinetic and diffusion study. *S Afr J Chem Eng.* 2020;32:39–55. doi:10.1016/j.sajce.2020.01.005
- [68] Al-Musawi TJ, Almajidi YQ, Al-Essa EM, et al. Levofloxacin adsorption onto MWCNTs/CoFe₂O₄ nanocomposites: mechanism, and modeling using Non-linear kinetics and isotherm equations. *Magnetochemistry.* 2023;9:9. doi:10.3390/magnetochemistry9010009
- [69] Guyo U, Phiri LY, Chigondo F. Application of central composite design in the adsorption of Ca(II) on metakaolin zeolite. *J Chem.* 2017; 1–10. doi:10.1155/2017/7025073
- [70] Wang J, Guo X. Adsorption isotherm models: classification, physical meaning, application and solving. *Chemosphere.* 2020;258:127279. doi:10.1016/j.chemosphere.2020.127279
- [71] Langmuir I. The constitution and fundamental properties of solids and liquids. *J Am Chem Soc.* 1916;38:2221–2295. doi:10.1021/ja02268a002
- [72] Langmuir I. The adsorption of gases on plane surfaces of glass, mica and platinum. *J Am Chem Soc.* 1918;40:1361–1403. doi:10.1021/ja02242a004
- [73] Freundlich HMF. Über die adsorption in lösungen. *Z Phys Chem.* 1906;57:385–470. doi:10.1515/zpch-1907-5723
- [74] Sips R. On the structure of a catalyst surface. *J Chem Phys.* 1948;16:490–495. doi:10.1063/1.1746922
- [75] Temkin MJ, Pyzhev V. Kinetics of ammonia synthesis on promoted iron catalyst. *Acta Phys Chim USSR.* 1940;12:327–356.
- [76] Brunauer S, Emmet PH, Teller E. Adsorption of gases in multimolecular layers. *J Am Chem Soc.* 1938;60:309–319. doi:10.1021/ja01269a023
- [77] Liu L, Luo X-B, Ding L, et al. Application of nanotechnology in the removal of heavy metal from water. In: X Luo, F Deng, editor. *Nanomaterials for the removal of pollutants and resource reutilization*. Amsterdam: Elsevier; 2019. p. 83–147. doi:10.1016/B978-0-12-814837-2.00004-4

- [78] Sritapunya T, Jairakdee S, Kornprapakul T, et al. Adsorption of surfactants on carbon black and paper fiber in the presence of calcium ions. *Colloids Surf A Physicochem: Eng Asp.* 2011;389(1-3):206–212. doi:10.1016/j.colsurfa.2011.08.025
- [79] Pal A, Pan S, Saha S. Synergistically improved adsorption of anionic surfactant and crystal violet on chitosan hydrogel beads. *Chem Eng J.* 2013;217:426–434. doi:10.1016/j.cej.2012.11.120
- [80] Mu T-H, Sun H-N. Sweet potato leaf polyphenols: preparation, individual phenolic compound composition and antioxidant activity. In: RR Watson, editor. *Polyphenols in plants (second edition)*. Amsterdam: Elsevier; 2019. p. 365–380. doi:10.1016/B978-0-12-813768-0.00022-0
- [81] Kyzas GZ, Peleka EN, Deliyanni EA. Nanocrystalline akaganite as adsorbent for surfactant removal from aqueous solutions. *Materials (Basel).* 2013;6(1):184–197. doi:10.3390/ma6010184
- [82] Huang LH, Sun YY, Yang T, et al. Adsorption behavior of Ni (II) on lotus stalks derived active carbon by phosphoric acid activation. *Desalination.* 2011;268(1-3):12–19. doi:10.1016/j.desal.2010.09.044
- [83] Kyzas GZ, McKay G, Al-Musawi TJ, et al. Removal of benzene and toluene from synthetic wastewater by adsorption onto magnetic zeolitic imidazole framework nanocomposites. *Nanomaterials.* 2022;12:3049. doi:10.3390/nano12173049
- [84] Kyzas GZ, Tolkou AK, Al Musawi TJ, et al. Fluoride removal from water by using green magnetic activated carbon derived from canola stalks. *Water Air Soil Pollut.* 2022;233:424. doi:10.1007/s11270-022-05900-6
- [85] Kalam S, Abu-Khamsin SA, Kamal MS, et al. Surfactant adsorption isotherms: A review. *ACS Omega.* 2021;6(48):32342–32348. doi:10.1021/acsomega.1c04661
- [86] Inyang M, Dickenson E. The potential role of biochar in the removal of organic and microbial contaminants from potable and reuse water: A review. *Chemosphere.* 2015;134:232–240. doi:10.1016/j.chemosphere.2015.03.072
- [87] Ntakirutimana S, Tan W, Wang Y. Enhanced surface activity of activated carbon by surfactants synergism. *RSC Adv.* 2019;9(45):26519. doi:10.1039/c9ra04521j
- [88] Veres P. FTIR Analysis of Particulate Matter Collected on Teflon Filters in Columbus, OH. Undergraduate thesis, The Ohio State University, 2005. Available online at: <https://research.cbc.osu.edu/allen.697/wp-content/uploads/2011/09/thesis-Veres-2005.pdf>.
- [89] Moussavi G, Shekoohiyan S, Mojab S. Adsorption capacity of NH₄Cl-induced activated carbon for removing sodium dodecyl sulfate from water. *Desal Water Treat.* 2016;57:11283–11290. doi:10.1080/19443994.2015.1043955
- [90] Bautista-Toledo MI, Mendez-Diaz JD, Sanchez-Polo M, et al. Adsorption of sodium dodecylbenzenesulfonate on activated carbons: effects of solution chemistry and presence of bacteria. *J Colloid Interface Sci.* 2008;317(1):11–17. doi:10.1016/j.jcis.2007.09.039